Overview of TMD results from Hall B at Jefferson Lab

H. Avakian (Jlab)

SPIN 2016, Sep 28, 2016

Outline

- Motivation
- SIDIS with CLAS
- Unpolarized target
  - event selection & binning
  - acceptance studies
  - radiative correction
- Polarized target
  - SSAs for pi0
  - DSAs for pi0
  - Dilution factor
  - Comparison with higher energies
- Dihadron production
- Summary

SIDIS: partonic cross sections

$$\nu = (qP)/M$$
$$Q^2 = (k - k')^2$$
$$y = (qP)/(kP)$$
$$x = Q^2/2(qP)$$
$$z = (qP_h)/(qP)$$

$$\sigma = F_{UU} + P_t F_{UL}^{\sin\phi} \sin 2\phi + P_b F_{LU}^{\sin\phi} \sin\phi \ldots$$

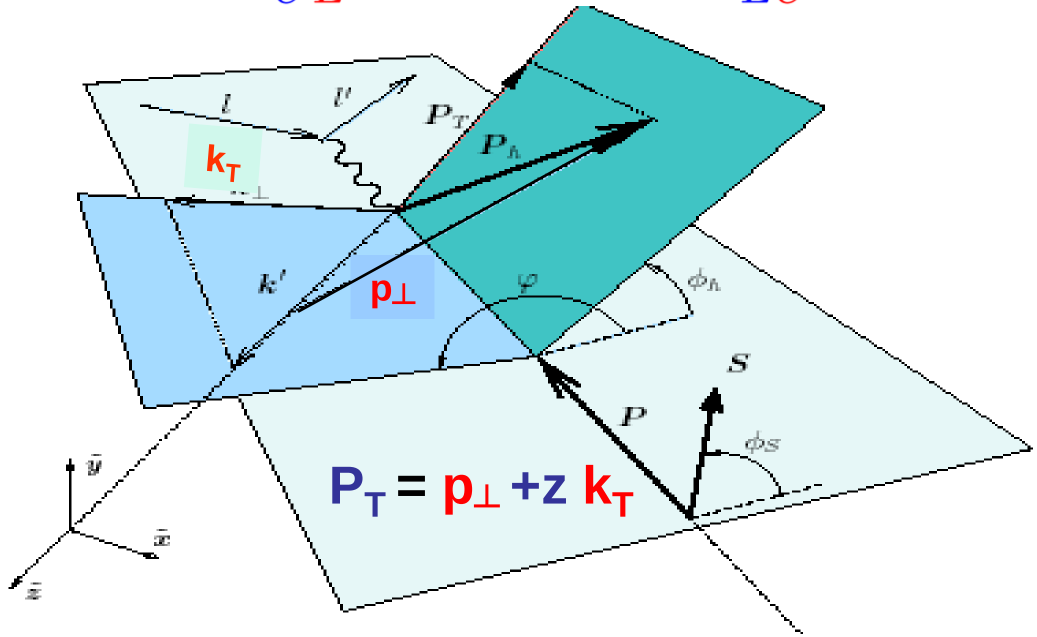

Transverse momentum of hadrons in SIDIS provides access to orbital motion of quarks

$$d\sigma^{\gamma^* H \to hX} \propto \sum e_q^2 \int d^2\vec{k}_T d^2\vec{p}_\perp f^{H\to q}(x, \vec{k}_T) D^{q\to h}(z, \vec{p}_\perp) \delta^{(2)}(z\vec{k}_T + \vec{p}_\perp - \vec{P}_T)$$

$$\Downarrow$$

$$d\sigma^h \propto \sum f^{H\to q}(x) \mathrm{d}\sigma_q(y) D^{q\to h}(z)$$

SIDIS ($\gamma^* p \to \pi X$) : k_T-dependences

$$\frac{d\sigma}{dx_B\,dy\,d\psi\,dz\,d\phi_h\,dP_{h\perp}^2} = \frac{\alpha^2}{x_B\,y\,Q^2}\,\frac{y^2}{2\,(1-\varepsilon)}\left(1+\frac{\gamma^2}{2x_B}\right)\Big\{F_{UU,T}+\varepsilon\,F_{UU,L}+\sqrt{2\,\varepsilon(1+\varepsilon)}\,\cos\phi_h\,F_{UU}^{\cos\phi_h}$$

$$+\,\varepsilon\cos(2\phi_h)\,F_{UU}^{\cos 2\phi_h}+\lambda_e\,\sqrt{2\,\varepsilon(1-\varepsilon)}\,\sin\phi_h\,F_{LU}^{\sin\phi_h}\Big\},$$

$f_1 \otimes D_1$

HT

HT

$h_1^\perp \otimes H_1^\perp$

HT

N/q	U	L	T
U	f_1		$h_1^\perp$
L		g_1	$h_{1L}^\perp$
T	$f_{1T}^\perp$	$g_{1T}^\perp$	h_1 $h_{1T}^\perp$

Pasquini&Yuan(2010)

BM TMD (1998) describes correlation between the transverse momentum and transverse spin of quarks, requires FSI or ISI

$$f_{q/p}(x,k_\perp^2) = \frac{1}{2}[f_1^q(x,k_\perp^2) - h_1^{\perp q}(x,k_\perp^2)\frac{(\hat{P}\times k_\perp)\cdot S_q}{M}]$$

$$h_1^{\perp q}(SIDIS) = -h_1^{\perp q}(DY)$$

BM TMD under intensive studies worldwide, including SIDIS and DY experiments, model calculations, lattice simulations.

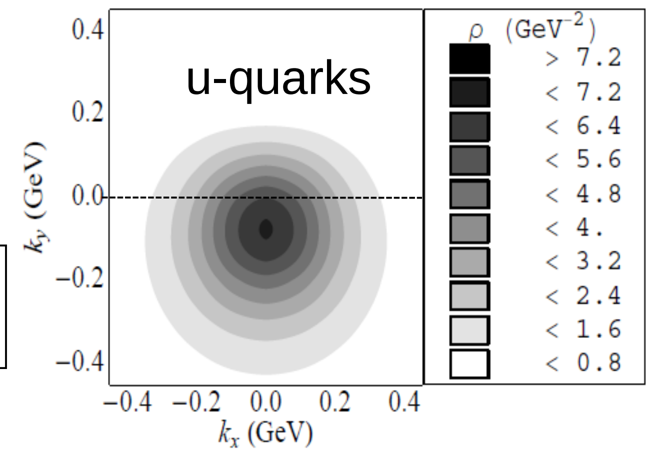

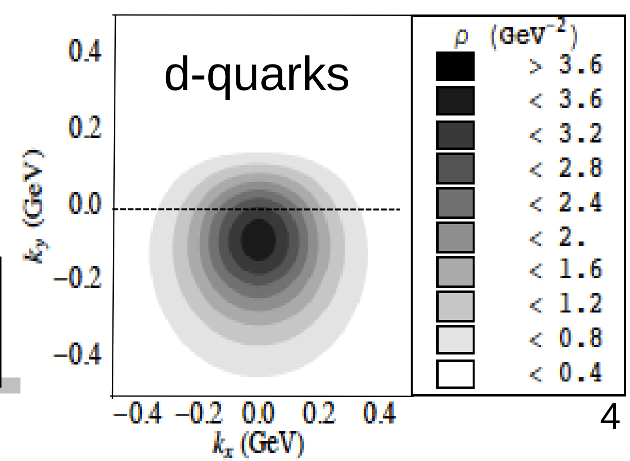

HT effects as background: Boer-Mulders distribution

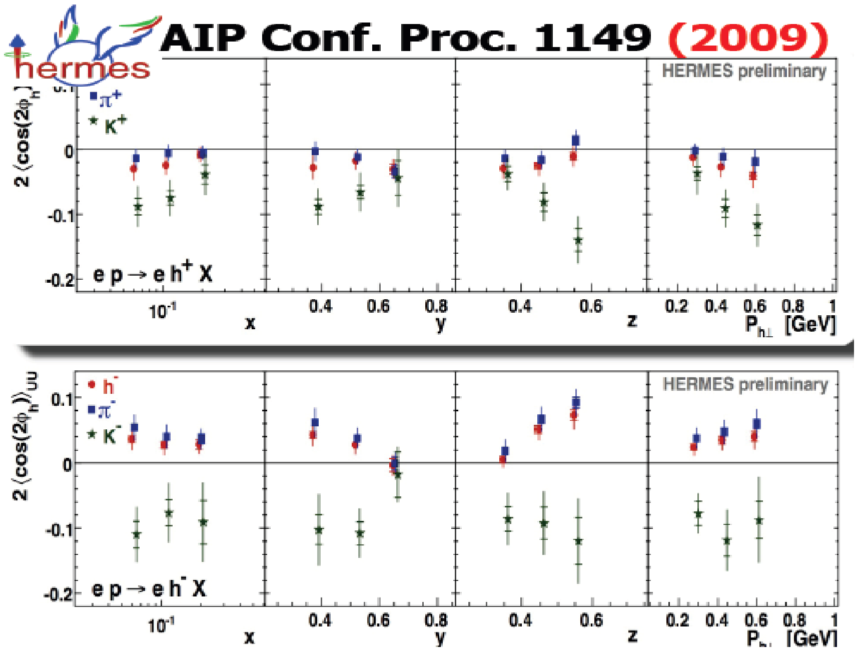

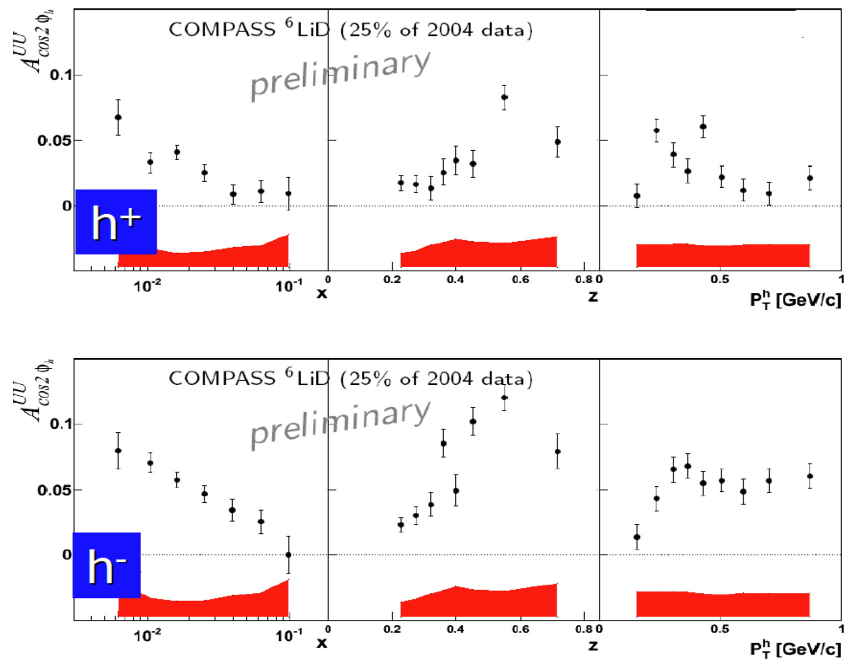

Background contributions :
Higher twist azimuthal moments
  kinematical HT (Cahn)
  dynamical HT (Berger-Brodsky)
Radiative correction
Acceptance

for cos2ϕ precision studies we need:
- Wide range in Q^2 and P_T (all background contributions are HT)
- Multidimensional binning
- Measurements with different final state hadrons

$$A_{UU}^{\cos 2\phi}(\pi^0) \approx A_{UU,Cahn}^{\cos 2\phi}$$

Azimuthal distributions in SIDIS

$$\frac{d\sigma}{dx_B\,dy\,d\psi\,dz\,d\phi_h\,dP_{h\perp}^2} = \frac{\alpha^2}{x_B y Q^2}\,\frac{y^2}{2\,(1-\varepsilon)}\left(1+\frac{\gamma^2}{2x_B}\right)\Big\{F_{UU,T}+\varepsilon F_{UU,L}+\sqrt{2\,\varepsilon(1+\varepsilon)}\,\cos\phi_h\,F_{UU}^{\cos\phi_h}$$

$$+\,\varepsilon\cos(2\phi_h)\,F_{UU}^{\cos 2\phi_h}+\lambda_e\sqrt{2\,\varepsilon(1-\varepsilon)}\,\sin\phi_h\,F_{LU}^{\sin\phi_h}\Big\},$$

$f_1 \otimes D_1$

h.t.

h.t.

$h_1^\perp \otimes H_1^\perp$

h.t.

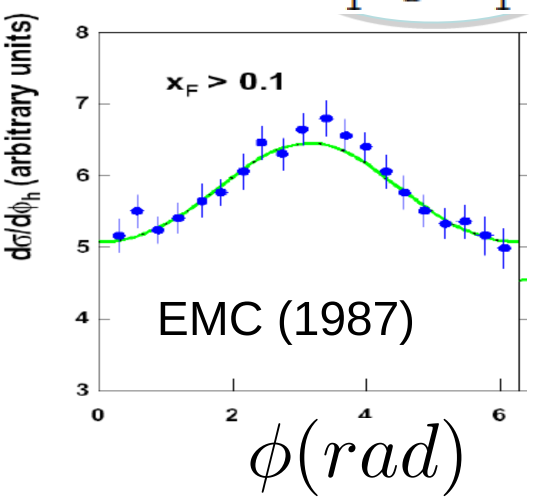

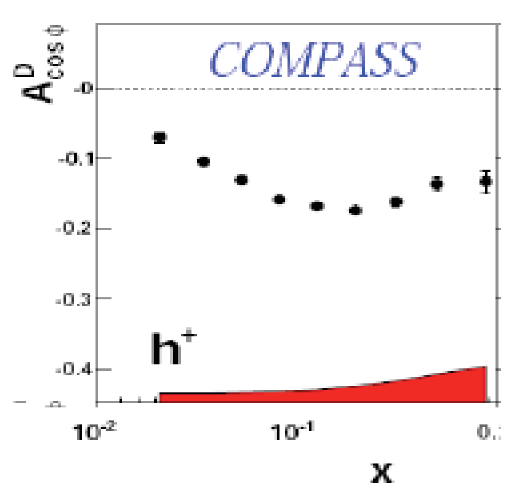

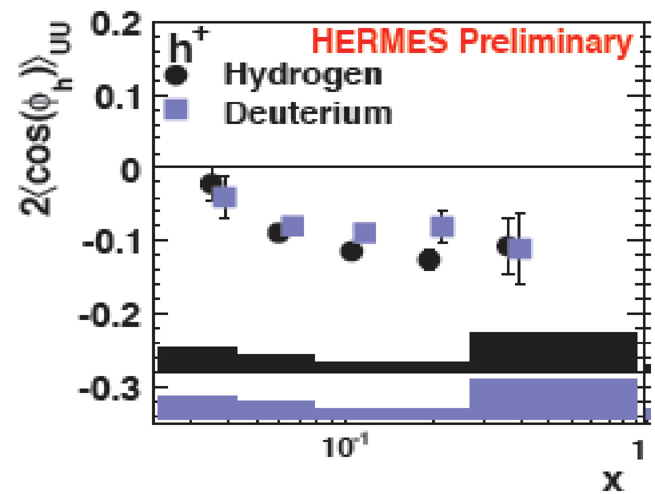

Understanding of cosϕ modulations observed by EMC, COMPASS and HERMES is crucial for interpretation of cos2ϕ and multiplicities

SIDIS cross-section

Expanding the contraction and integrating over ψ and the beam polarization, the cross-section for an unpolarized target can be written as

$$\frac{d^5\sigma}{dx\ dQ^2\ dz\ d\phi_h\ dP_{h\perp}^2} =$$

$$\underbrace{\frac{2\pi\alpha^2}{xyQ^2}\frac{y^2}{2(1-\epsilon)}\left(1+\frac{\gamma^2}{2x}\right)(F_{UU,T}+\epsilon F_{UU,L})}_{A_0}\left\{1+\underbrace{\frac{\sqrt{2\epsilon(1+\epsilon)}F_{UU}^{\cos\phi_h}}{(F_{UU,T}+\epsilon F_{UU,L})}}_{A_{UU}^{\cos\phi_h}}\cos\phi_h+\underbrace{\frac{\epsilon F_{UU}^{\cos 2\phi_h}}{(F_{UU,T}+\epsilon F_{UU,L})}}_{A_{UU}^{\cos 2\phi_h}}\cos 2\phi_h\right\}$$

According the the factorization theorem, structure functions can, in the Bjorken limit, be written as convolutions of TMDs and FFs $F = \sum \mathrm{TMD} \otimes \mathrm{FF}$

Bjorken Limit:

$$Q^2 \to \infty$$

$$2P \cdot q \to \infty$$

$$P \cdot P_h \to \infty$$

$$\text{fixed}\begin{cases} x = Q^2/2P \cdot q \\ z = P \cdot P_h/P \cdot q \end{cases}$$

CLAS data sets

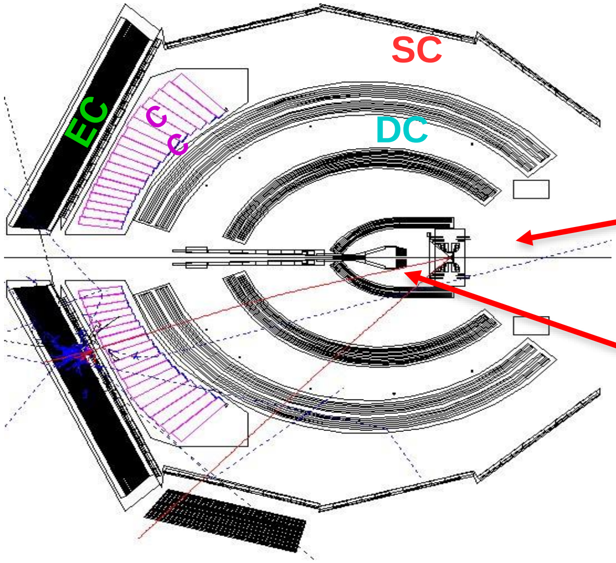

Hall B

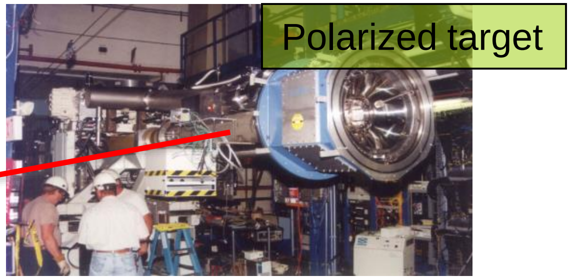

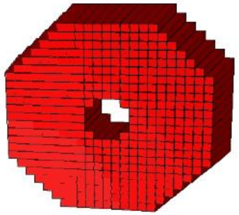

424 $PbWO_4$

Inner Calorimeter

- Electromagnetic Calorimeter (EC) and Čerenkov Counter (CC) used in electron identification.

- Drift Chamber (DC) (3 regions) and time of flight Scintillators (SC) record position and timing information for each charged track.

- Torus magnet creates toroidal magnetic field which causes charged tracks to curve while preserving the φ_{lab} angle.

- Continuous, polarized electron beam up to 6 GeV delivered simultaneously to 3 experimental halls.
- High luminosity of 0.5 x 10^{34} $(cm^2\ s)^{-1}$

$$ep \to e'\pi^{\pm}X$$

-E1-f run: 5.498 GeV electron beam with ~75% polarization (averaged over for this analysis); unpolarized liquid hydrogen target, 2 billion events;

$$ep \to e'\pi^{0}X$$

-Eg1dvcs run: 5.8 GeV electrons and protons ($^{14}NH_3$) polarized ~80%, 4.3M events

SIDIS Cuts and Binning

π+ channel   π- channel

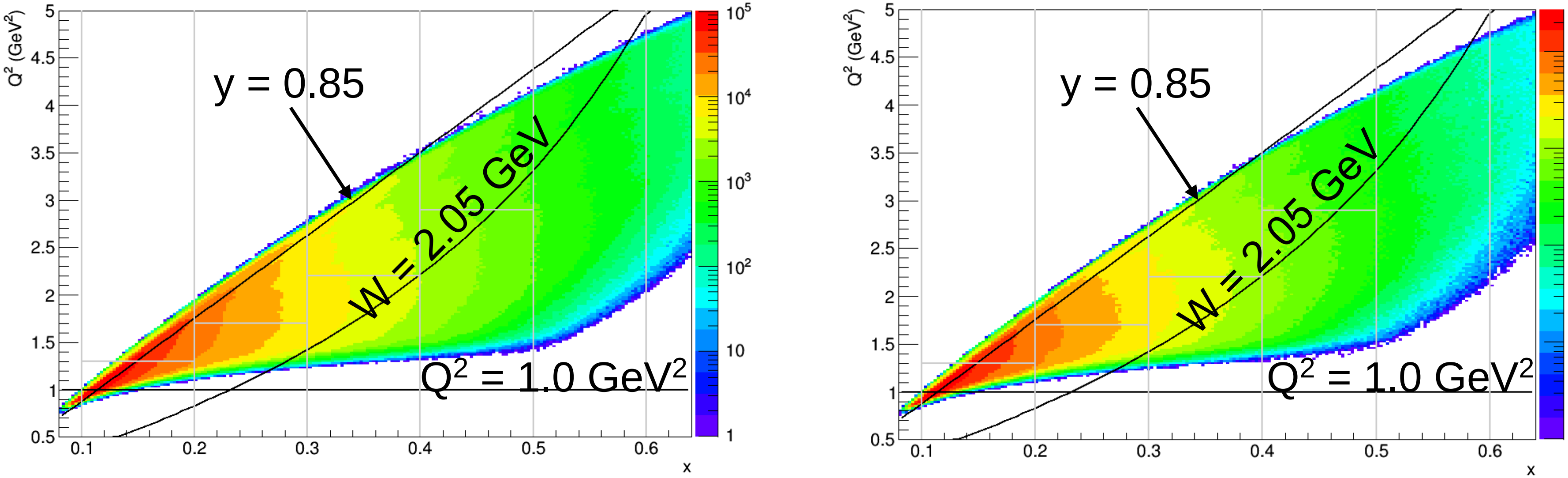

The DIS region is defined as Q^2 > 1.0 GeV^2 and W > 2.05 GeV.

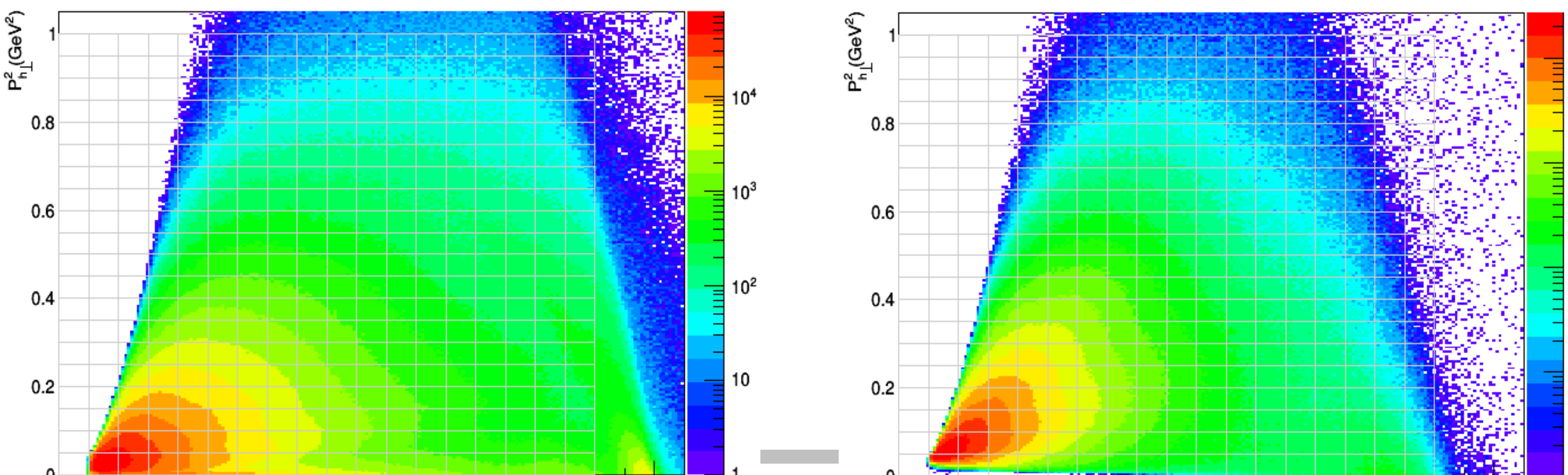

Monte Carlo φ generated, reconstructed, and acceptance for π+ (lowest x-Q^2 bin)

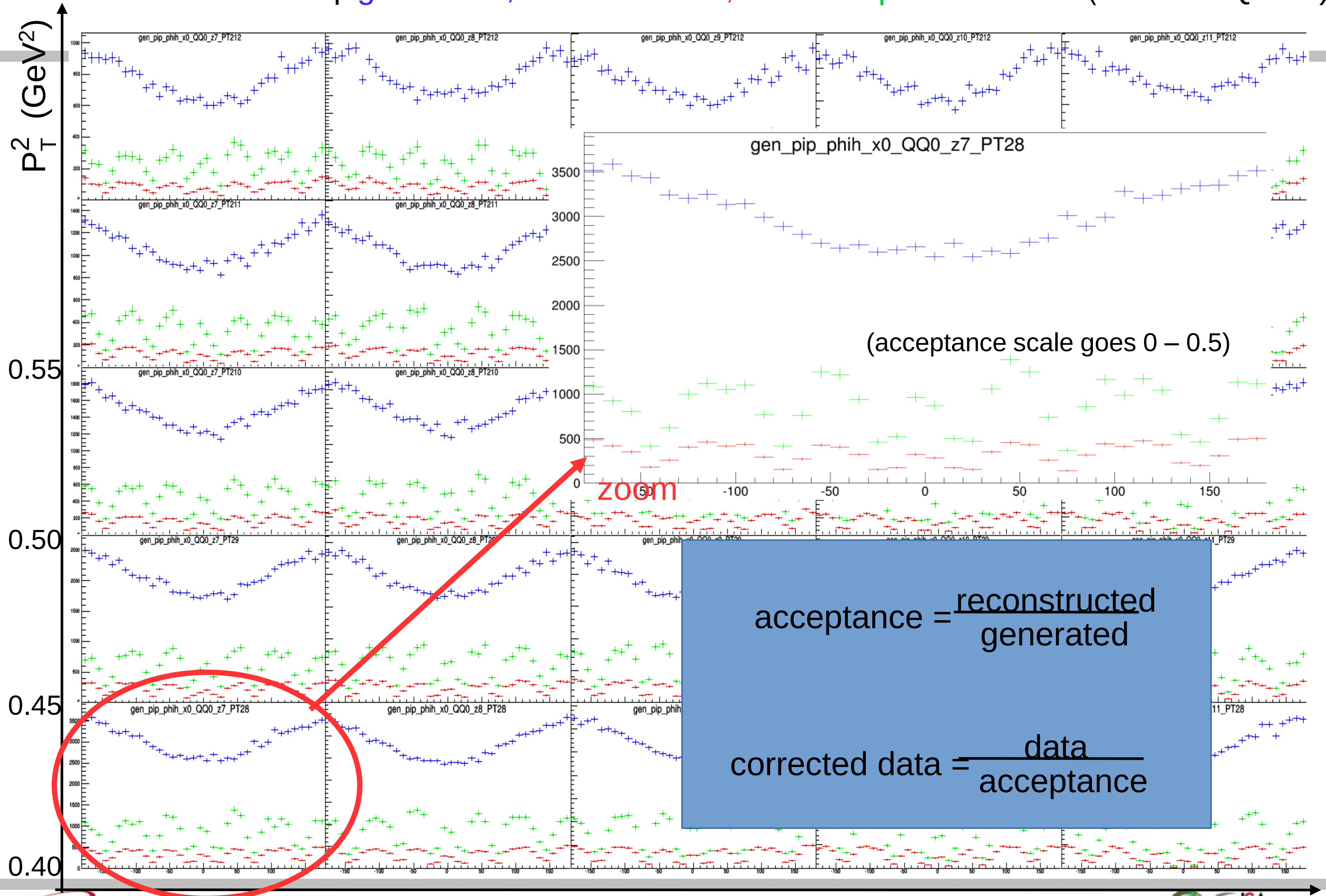

$$\text{acceptance} = \frac{\text{reconstructed}}{\text{generated}}$$

$$\text{corrected data} = \frac{\text{data}}{\text{acceptance}}$$

Born, radiated, and exclusive tail cross-sections from HAPRAD (lowest x-Q^2 bin)

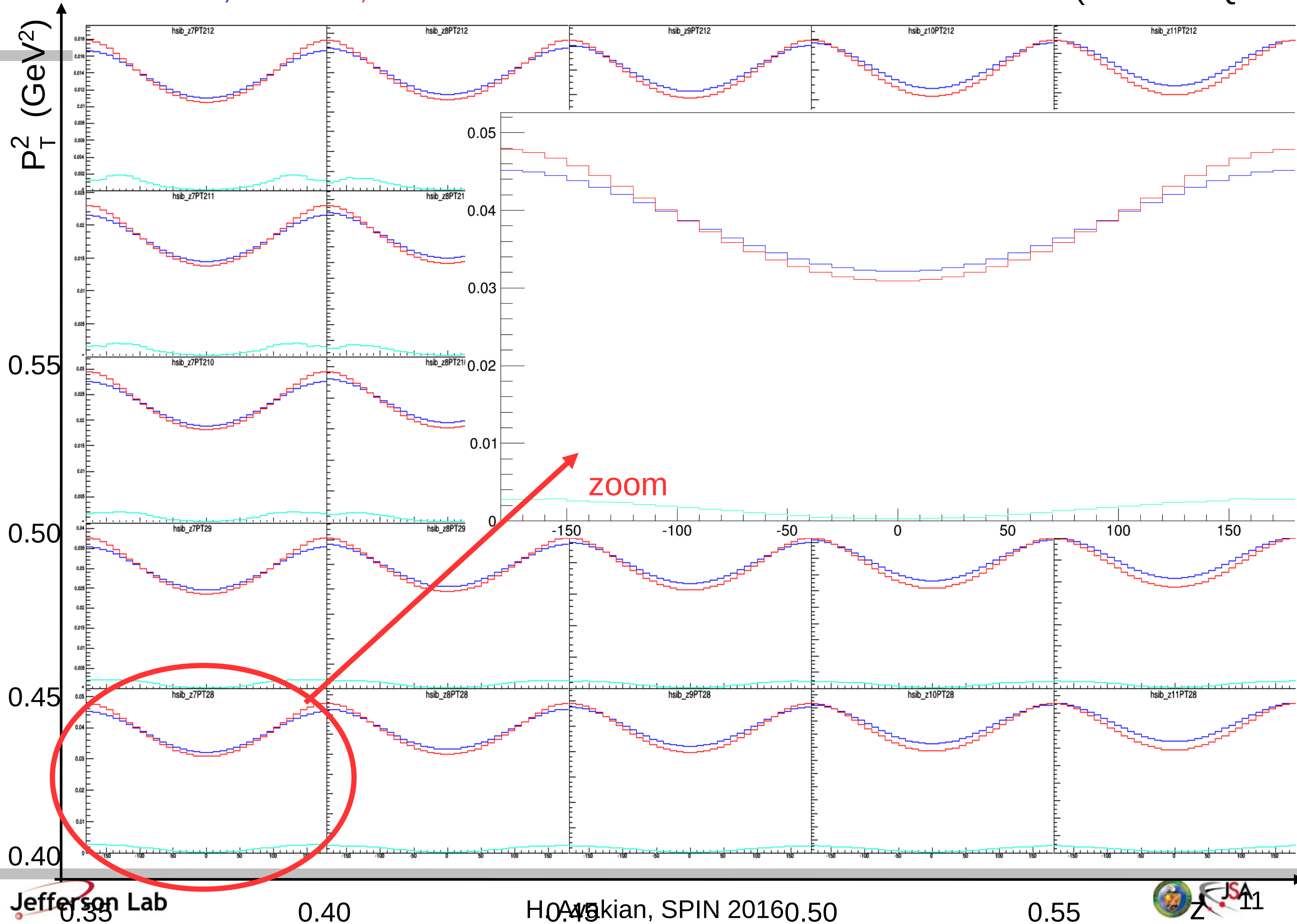

φ_h distributions – acceptance and radiative corrected with fit results (lowest x-Q^2 bin)

N. Harrison

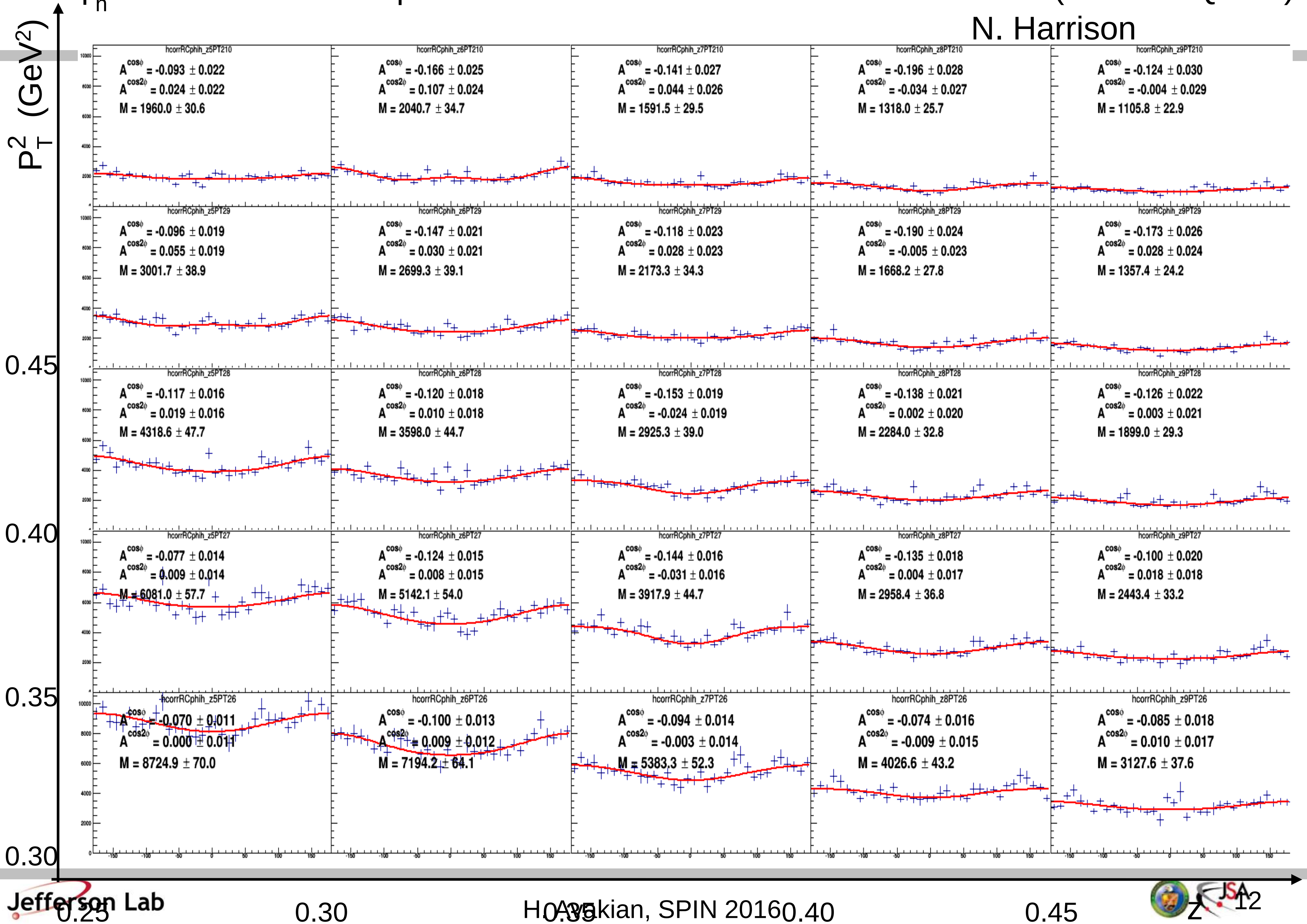

Measuring SIDIS cross section

Fit with $a(1 + b\cos\phi_h + c\cos 2\phi_h)$

N. Harrison

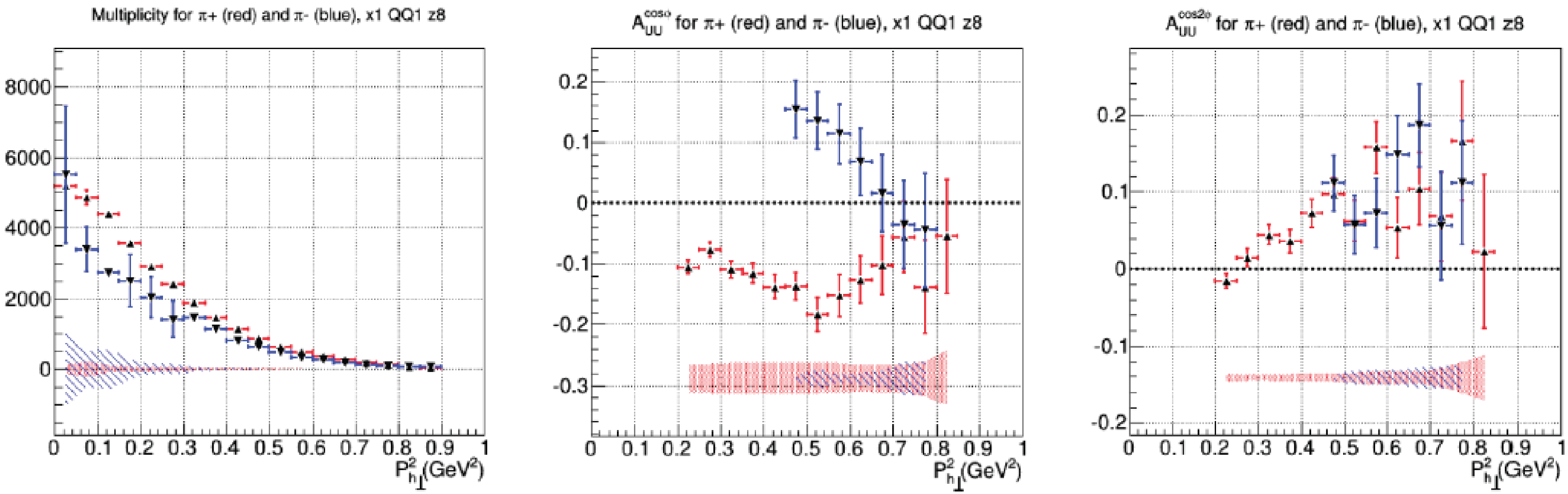

in WW approximation

$$F_{UU}^{\cos\phi_h} = \frac{2M}{Q}\,\mathcal{C}\left[\frac{\hat{h}\cdot p_\perp}{zM_h}\frac{k_\perp^2}{M^2}h_1^\perp H_1^\perp - \frac{\hat{h}\cdot k_\perp}{M} z f_1 D_1\right]$$

Simetric behaviour indicates large BM contribution

Extracting the average transverse momenta

Andrea Signori,[1,*] Alessandro Bacchetta,[2,3,†] Marco Radici,[3,‡] and Gunar Schnell[4,5,§]

$$F_{UU,T}(x,z,P_{hT}^2,Q^2) = \sum_a \mathcal{H}^a_{UU,T}(Q^2;\mu^2) \int dk_\perp\, dP_\perp\, f_1^a(x,k_\perp^2;\mu^2)\, D_1^{a\to h}(z,P_\perp^2;\mu^2)\, \delta(zk_\perp - P_{hT} + P_\perp) + Y_{UU,T}(Q^2,P_{hT}^2) + \mathcal{O}(M/Q).$$

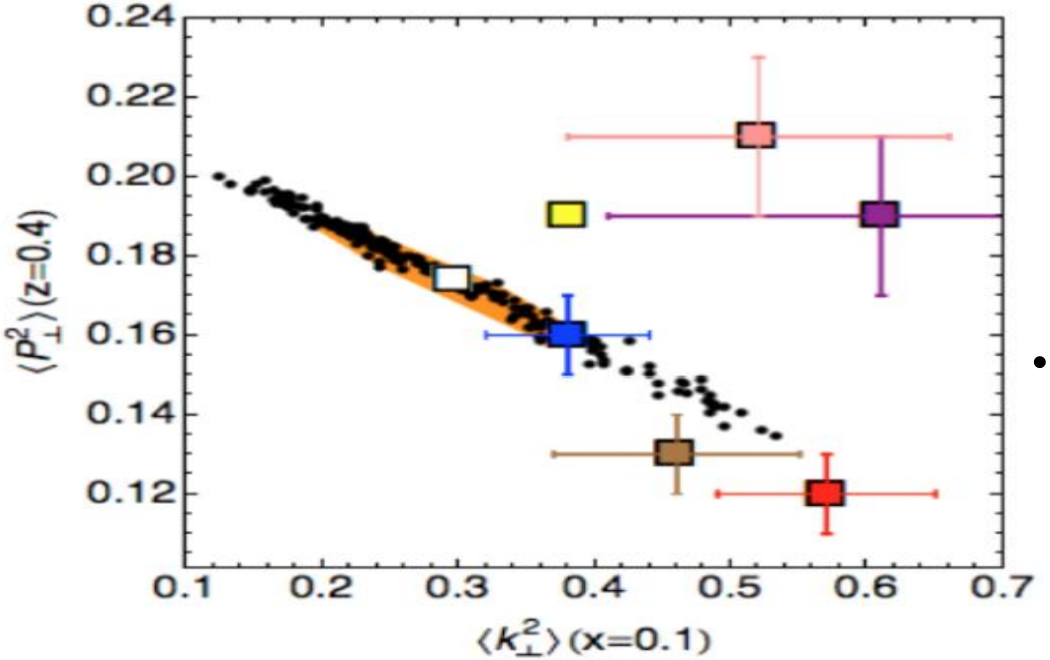

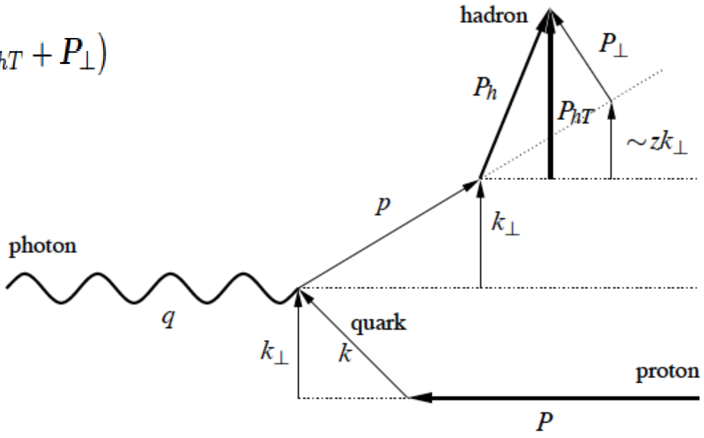

- Multiplicity alone may not be enough to separate $\langle k_T \rangle$ from average $\langle p_T \rangle$

$$m_N^h(x,z,P_{hT}^2) = \frac{\pi}{\sum_a e_a^2 f_1^a(x)} \times \sum_a e_a^2\, f_1^a(x)\, D_1^{a\to h}(z)\, \frac{e^{-P_{hT}^2/\left(z^2\langle k_{\perp,a}^2\rangle + \langle P_{\perp,a\to h}^2\rangle\right)}}{\pi\left(z^2\langle k_{\perp,a}^2\rangle + \langle P_{\perp,a\to h}^2\rangle\right)}$$

$$\frac{\left(F_{UU}^{\cos\phi_h}\right)_{Cahn}}{F_{UU}} \propto \frac{\langle k_\perp^2 \rangle}{\langle P_T^2 \rangle}$$

- cos ϕ has much greater sensitivity to $\langle k_T \rangle$

k_T-max effects on observables

M. Boglione, S. Melis & A. Prokudin **Phys. Rev. D 84, 034033 2011**

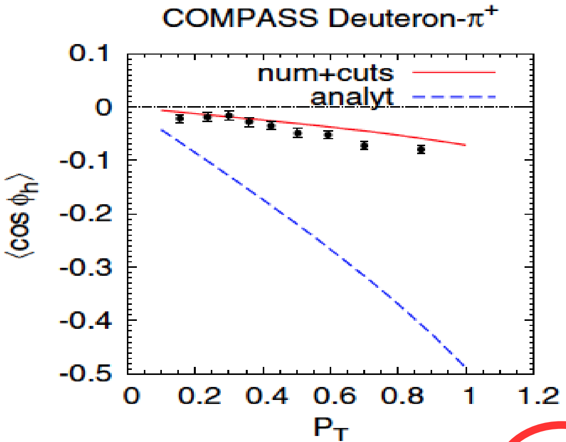

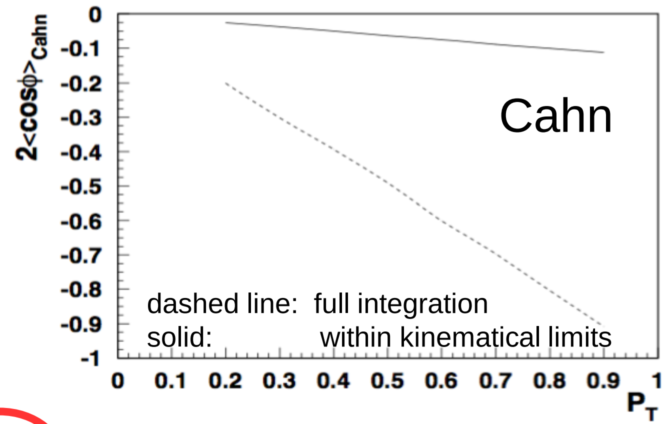

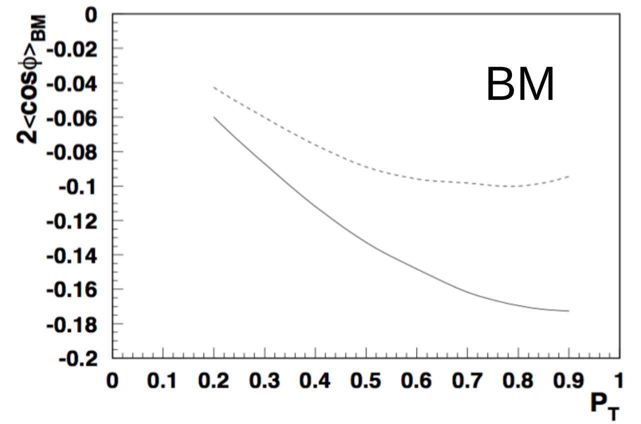

$$\mathcal{C}[w, fD] = x \sum_a e_a^2 \int_0^{k_{\perp max}} k_\perp dk_\perp \int_0^{2\pi} d\phi \, w(\boldsymbol{k}_\perp, \boldsymbol{p}_\perp(\boldsymbol{k}_\perp)) f^a(x, k_\perp^2) \, D^a(z, (\boldsymbol{P}_{h\perp} - z\boldsymbol{k}_\perp)^2)$$

in WW approximation

$$F_{UU}^{\cos\phi_h} = \frac{2M}{Q} \mathcal{C}\left[\frac{\hat{h}\cdot p_\perp}{zM_h} \frac{k_\perp^2}{M^2} h_1^\perp H_1^\perp - \frac{\hat{h}\cdot k_\perp}{M} z f_1 D_1 \right]$$

BM contribution seem to be less sensitive to phase space limitations

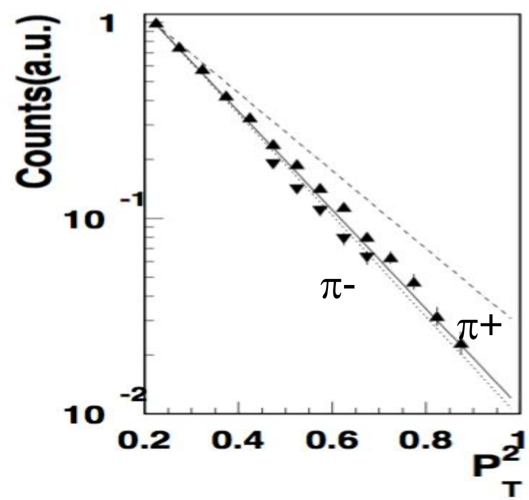

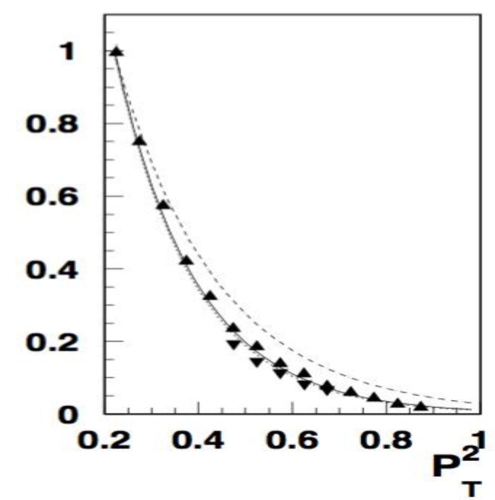

multiplicities are also sensitive to kinematic limitations

Comparing with HERMES

$$F_{UU,T} + \varepsilon F_{UU,L} + \sqrt{2\,\varepsilon(1+\varepsilon)}\cos\phi_h\, F_{UU}^{\cos\phi_h}$$

$$F_{UU}^{\cos\phi_h} = \frac{2M}{Q}\mathcal{C}\left[\frac{\hat{h}\cdot p_\perp}{zM_h}\frac{k_\perp^2}{M^2}h_1^\perp H_1^\perp - \frac{\hat{h}\cdot k_\perp}{M} z f_1 D_1\right],$$

CLAS data consistent with HERMES (27.5 GeV)
π- above π+!

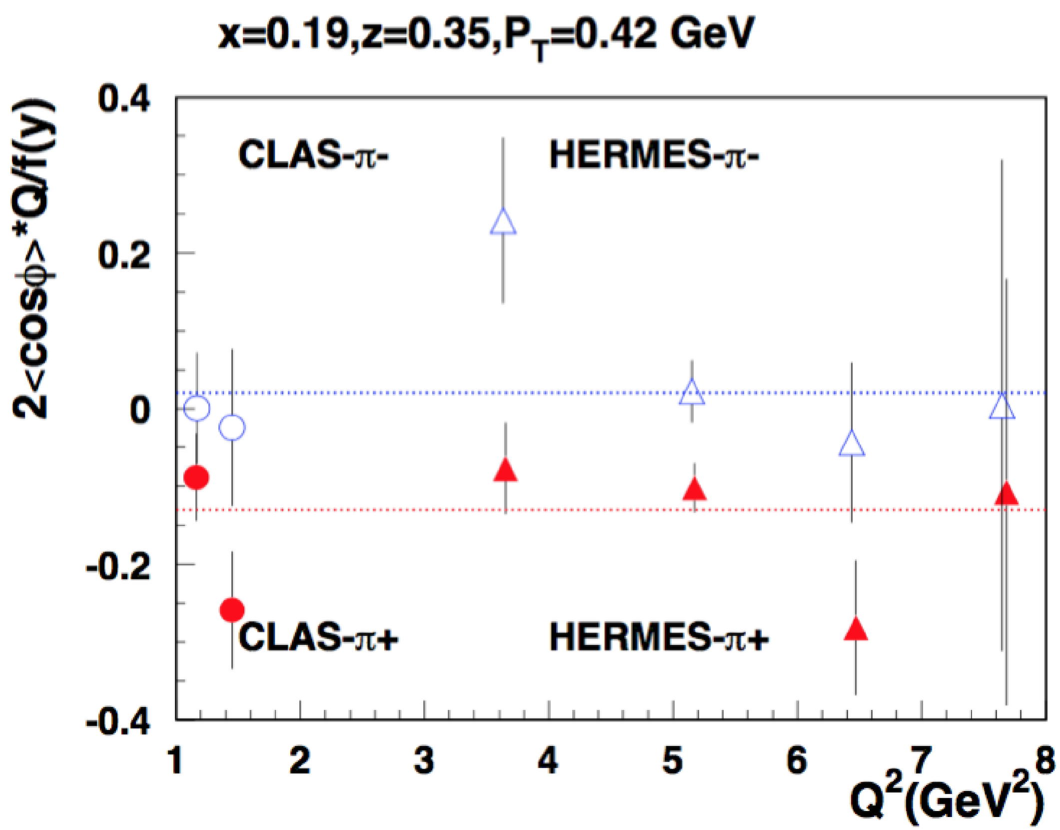

Polarized target: Dilution factor in SIDIS

$$f_{DF} = \frac{B_{NH_3}\sigma_p}{A_{NH_3}\sigma + B_{NH_3}\sigma_p}$$

$$\frac{n_{NH_3}}{n_C} = \frac{A_{NH_3}}{A_C} + \frac{B_{NH_3}}{A_C}\frac{\sigma_p}{\sigma}$$

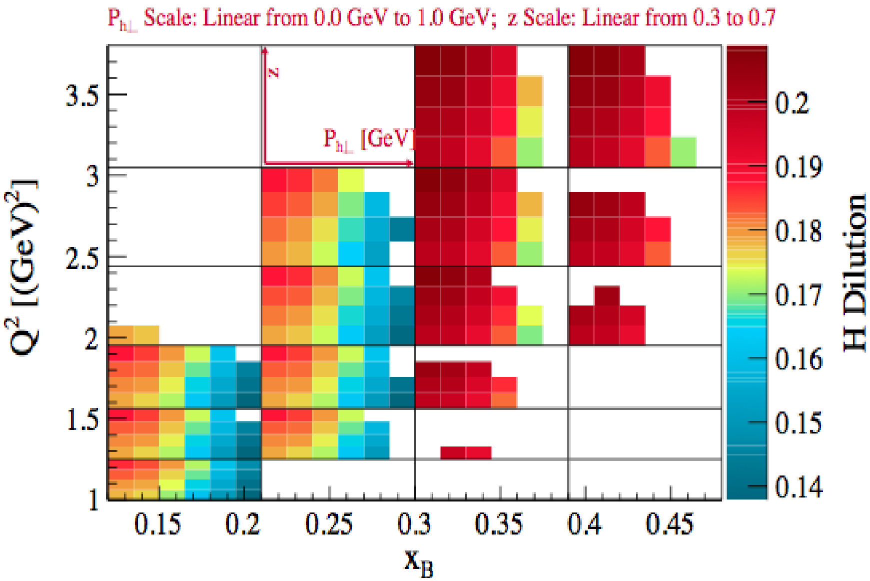

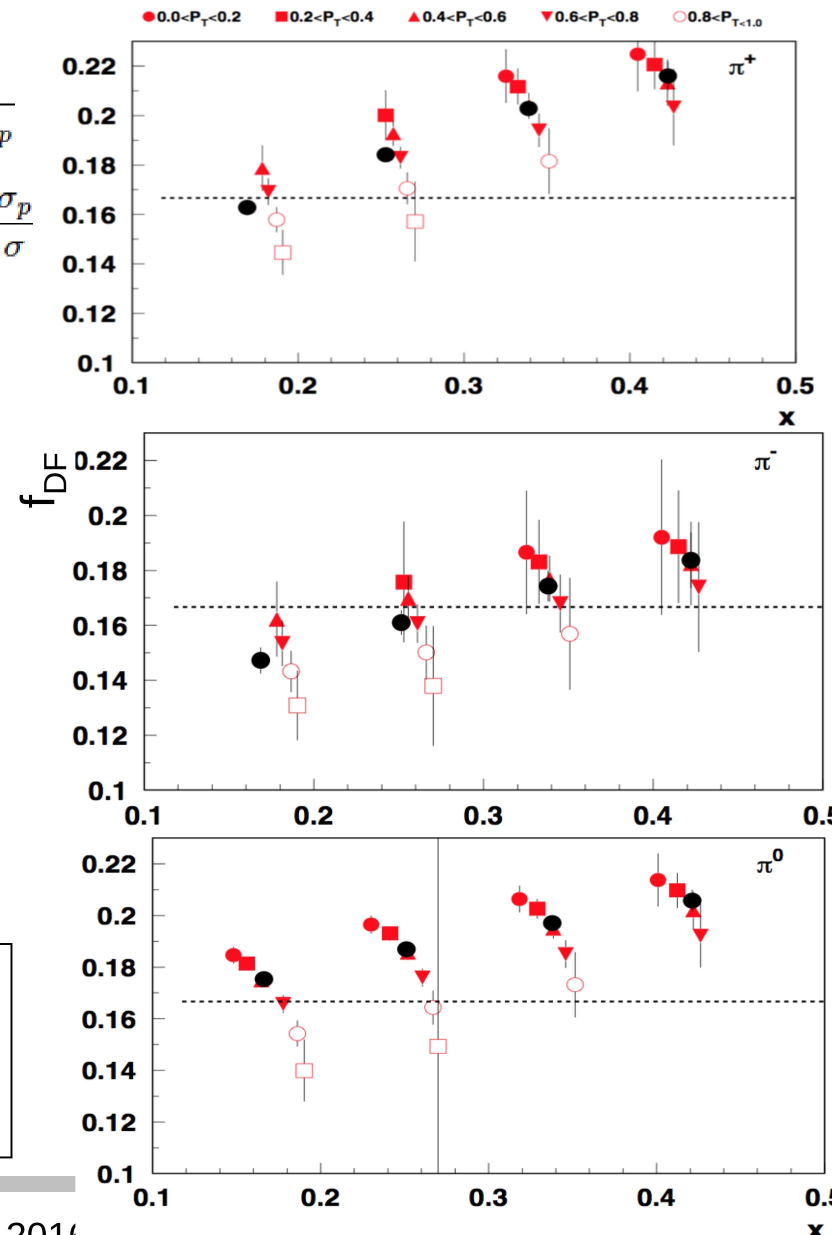

Understanding the dilution factor is a major effort in precision multidimensional analysis, for multiparticle final states

$A_{UL}^{\sin\phi}$, $A_{LL}^{\cos\phi}$: First measurement & possible interpretation

$$ep \rightarrow e'\pi^0 X$$

$$A_{UL}^{\sin\phi} \propto f_L^{\perp} D_1 + h_L H_1^{\perp}$$

N/q	U	L	T
U	$f^{\perp}$	$g^{\perp}$	h, e
L	$f_L^{\perp}$	$g_L^{\perp}$	h_L, e_L
T	$f_T, f_T^{\perp}$	$g_T, g_T^{\perp}$	$h_T, e_T, h_T^{\perp}, e_T^{\perp}$

q/h	U
U	D_1
L	
T	$H_1^{\perp}$

$$A_{LL}^{\cos\phi} \propto g_L^{\perp} D_1 + e_L H_1^{\perp}$$

W.Mao et al, Nucl.Phys. A945 (2016) 153-167

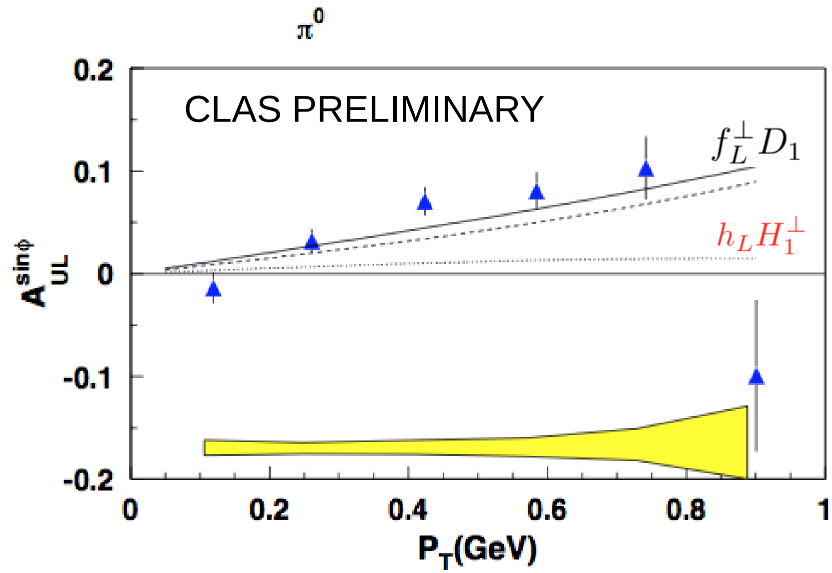

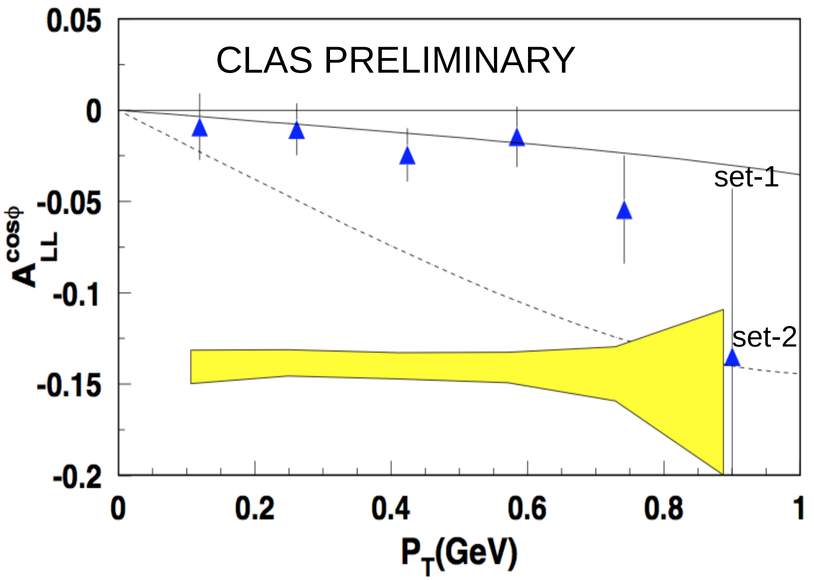

π^0 SSA less sensitive to polarized fragmentation effects (Collins function suppressed)

Double spin asymmetry vs x

$$\sigma_p^{eX} \propto 4u + d + \ldots$$

$$\Delta\sigma_p^{eX} \propto 4\Delta u + \Delta d + \ldots$$

$$\sigma_p^{\pi^0} \propto 4uD^{u\to\pi^0} + dD^{d\to\pi^0} + \ldots$$

$$\Delta\sigma_p^{\pi^0} \propto 4\Delta uD^{u\to\pi^0} + \Delta dD^{d\to\pi^0} + \ldots$$

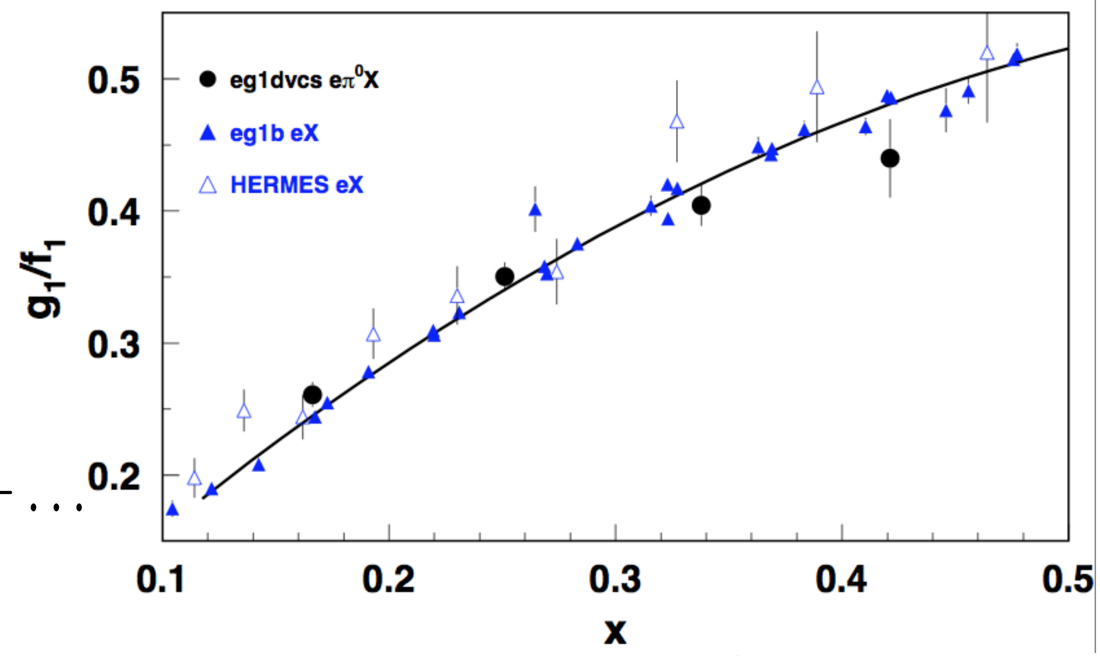

$$g_1^p/f_1^p(eX) \approx g_1^p/f_1^p(e\pi^0 X) \approx (4\Delta u + \Delta d)/(4u + d)$$

$$A_{\parallel} \approx \frac{(1-\varepsilon)(2-y)}{y\,(1+\varepsilon R)}\,\frac{g_1}{F_1} \equiv \frac{y(2-y)}{y^2 + 2\left(1 - y - \frac{y^2\gamma^2}{4}\right)\frac{(1+R)}{(1+\gamma^2)}}\frac{g_1}{F_1} \equiv D'(y)\frac{g_1}{F_1}$$

averaged over P_T x-dependence of g_1/f_1 for $\pi 0$ consistent with inclusive asymmetry.

g_1/f_1: P_T-dependence for x-bins

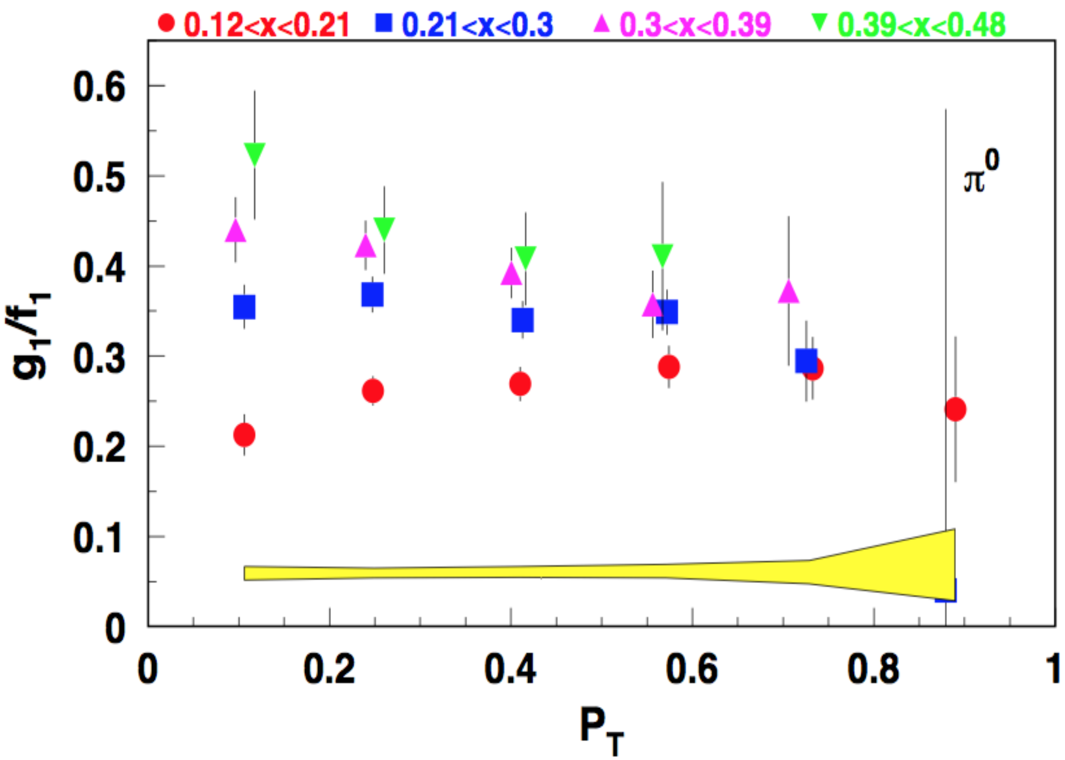

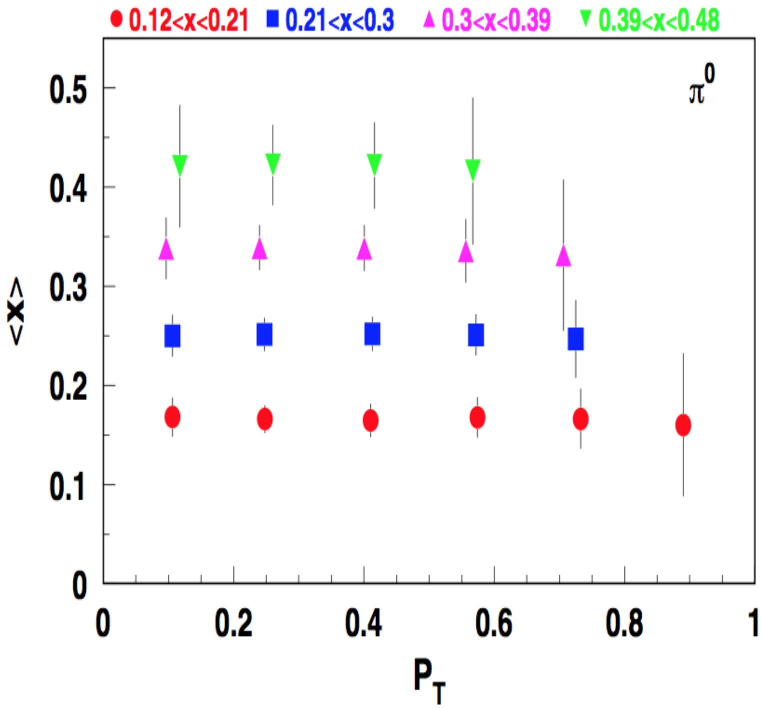

1) Simple PID by π^0-mass (no kaon contamination)
2) SIDIS π^0 production is not contaminated by diffractive ρ
3) Less contaminated by resonance production
4) HT effects and exclusive π^0 suppressed
5) Provides information complementary to $\pi^{+/-}$ information on PDFs
6) π^0 SSA less sensitive polarized fragmentation effects (Collins function suppressed)

g_1/f_1: accessing k_T-dependence of polarized quarks

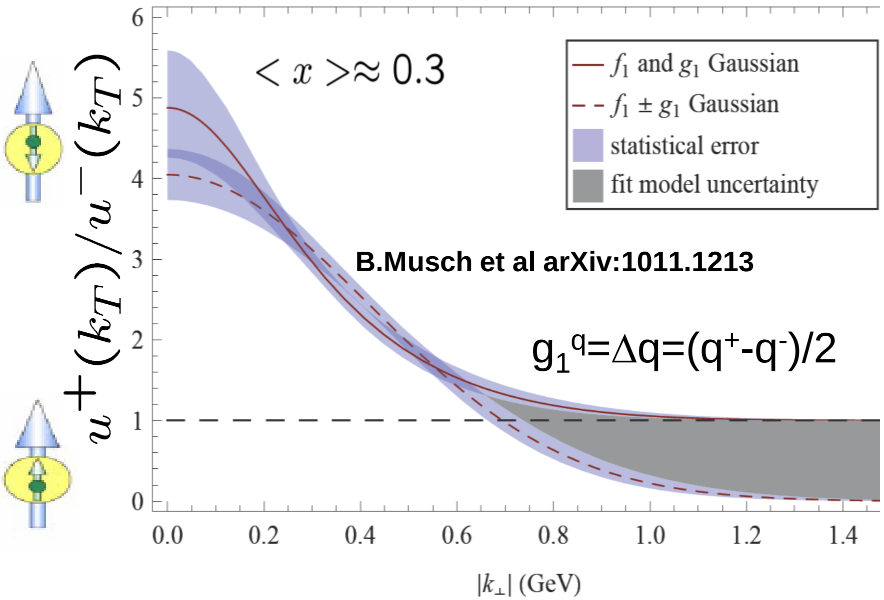

M.Anselmino et al **hep-ph/0608048**

$$f_1^q(x, k_T) = f_1(x) \frac{1}{\pi \mu_0^2} \exp\left(-\frac{k_T^2}{\mu_0^2}\right)$$

$$g_1^q(x, k_T) = g_1(x) \frac{1}{\pi \mu_2^2} \exp\left(-\frac{k_T^2}{\mu_2^2}\right)$$

$$D_1^q(z, p_T) = D_1(z) \frac{1}{\pi \mu_D^2} \exp\left(-\frac{p_T^2}{\mu_D^2}\right)$$

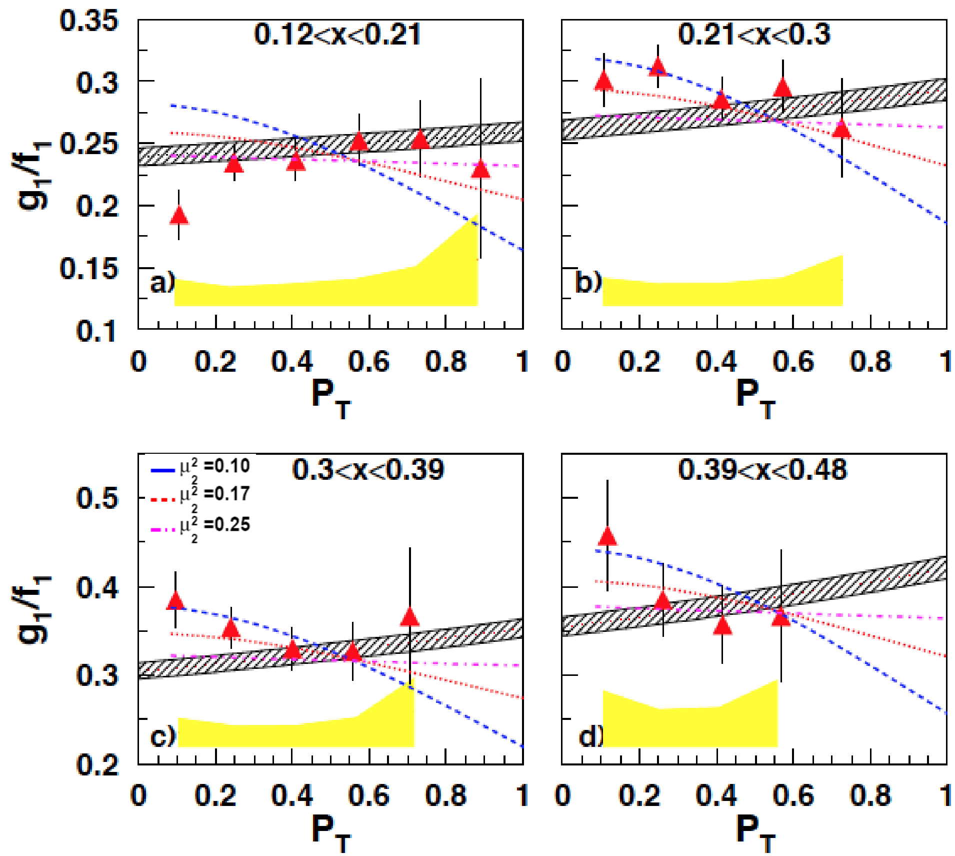

Bourrely & Soffer
Nuclear Physics A 941 (2015) 307–334

μ_0^2=0.25GeV^2
μ_D^2=0.2GeV^2

P_T-dependence of the double spin asymmetry provides access to k_T-dependence of polarized quarks

$ep \to e'\pi^0 X$

Kotzinian-Mulders asymmetry

N \ q	U	L	T
U	f_1		$h_1^\perp$
L		g_1	$\boxed{h_{1L}^\perp}$
T	$f_{1T}^\perp$	g_{1T}	h_1 $h_{1T}^\perp$

$A_{UL}^{\sin 2\phi} \sim h_{1L}^\perp H_1^\perp \sin 2\phi$

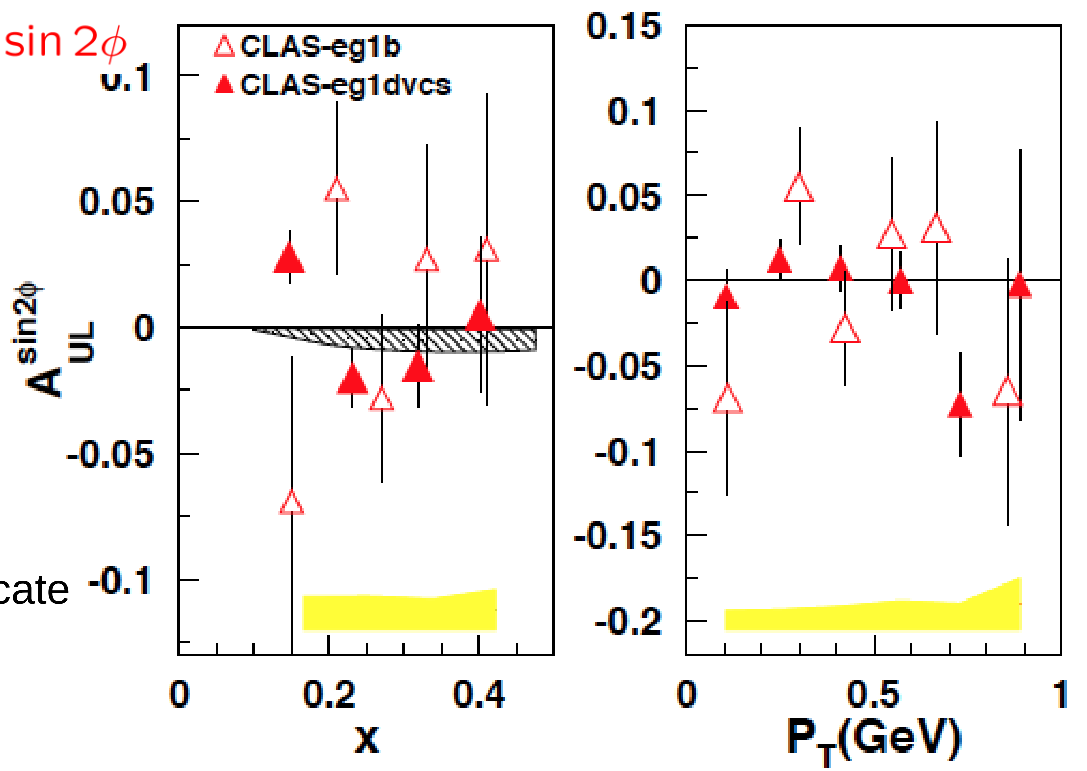

Fragmentation of transversely polarized quarks to π^0

Hermes/Belle measurements for pions indicate

$$H_1^{\perp fav} \approx -H_1^{\perp unfav}$$

New precision data for π^0 is consistent with suppression of SSA due to opposite sign for favored and unfavored Collins fragmentation functions(H_1)

Hadron production in hard scattering

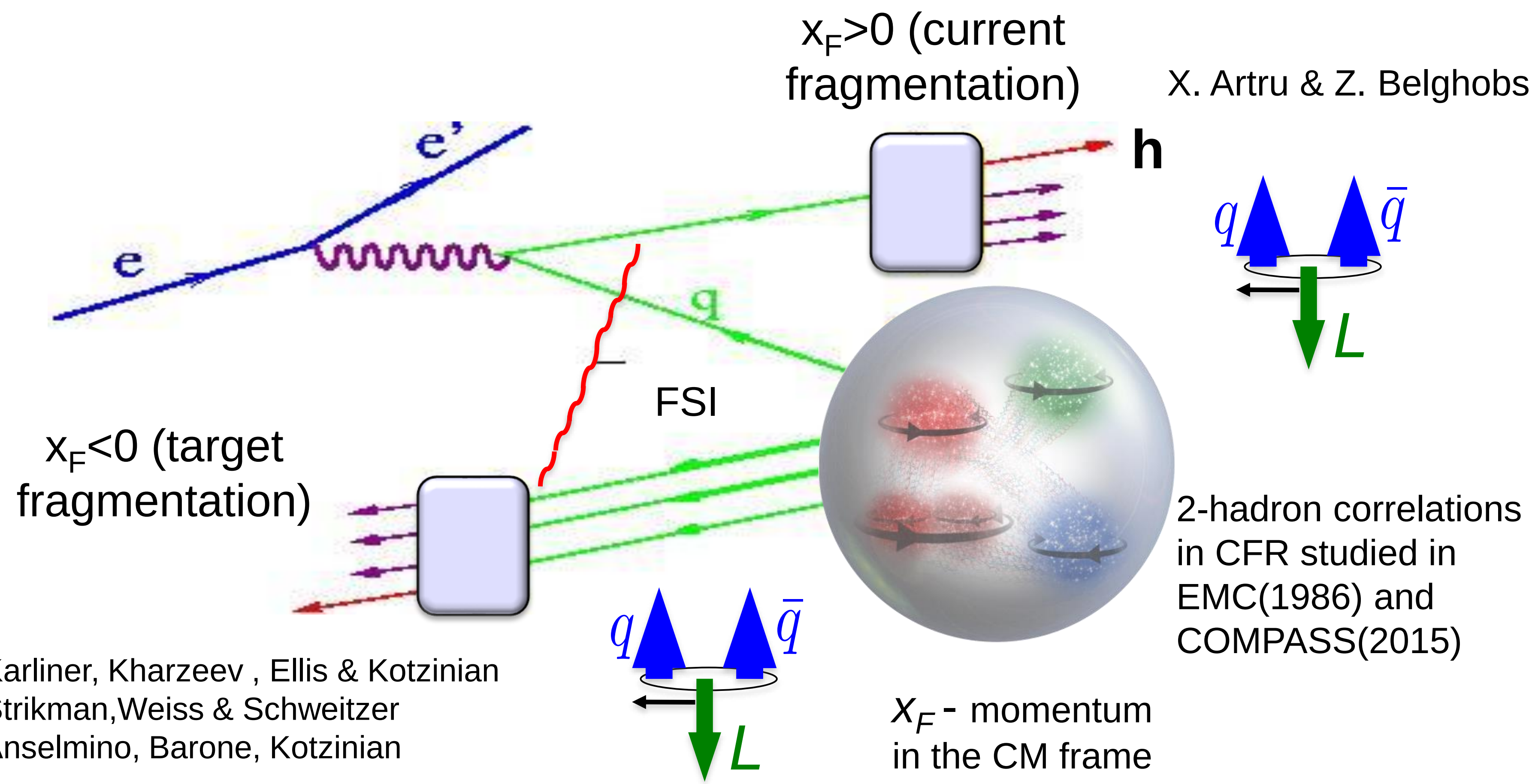

Karliner, Kharzeev , Ellis & Kotzinian
Strikman,Weiss & Schweitzer
Anselmino, Barone, Kotzinian

Correlations of the spin of the target or/and the momentum and the spin of quarks, combined with final state interactions define the azimuthal distributions of produced particles

Back-to-back hadron (b2b) production in SIDIS

P$_1$

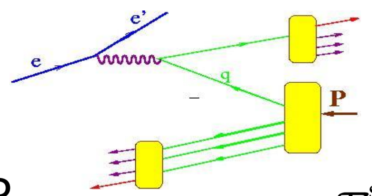

P$_2$

M. Anselmino, V. Barone and A. Kotzinian,
Physics Letters B 713 (2012)

$$\mathcal{F}_{LU}^{\sin(\phi_1-\phi_2)} = \frac{|\vec{P}_{1\perp}\vec{P}_{2\perp}|}{m_N m_2} \mathcal{C}[w_5 M_L^{\perp,h} D_1]$$

Leading Twist

	U	L	T
U	M	$M_L^{\perp,h}$	$M_T^h, M_T^\perp$
L	$\Delta M^{\perp,h}$	ΔM_L	$\Delta M_T^h, \Delta M_T^\perp$
T	$\Delta_T M_T^h, \Delta_T M_T^\perp$	$\Delta_T M_L^h$ $\Delta_T M_L^\perp$	$\Delta_T M_T, \Delta_T M_T^{hh}$ $\Delta_T M_T^{\perp\perp}, \Delta_T M_T^{\perp h}$

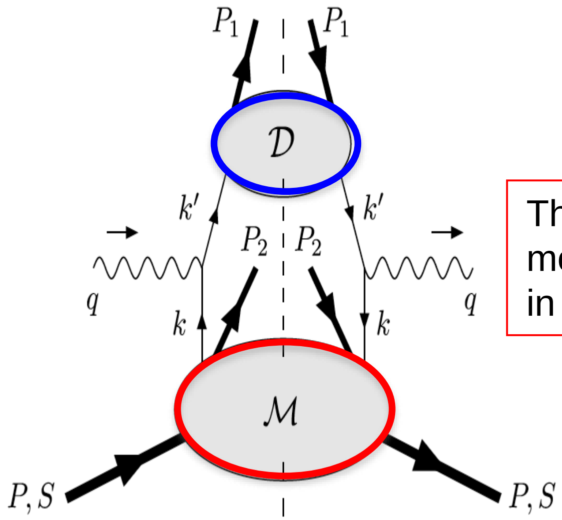

The beam–spin asymmetry appears, at leading twist and low transverse momenta, in the deep inelastic inclusive lepto-production of two hadrons, one in the target fragmentation region and one in the current fragmentation region.

$$A_{LU} = -\frac{y\left(1-\frac{y}{2}\right)}{\left(1-y+\frac{y^2}{2}\right)} \frac{\mathcal{F}_{LU}^{\sin\Delta\phi}}{\mathcal{F}_{UU}} \sin\Delta\phi$$

Back-to-back hadron production in SIDIS would allow:
- study SSAs not accessible in SIDIS at leading twist
- measure fracture functions
- control the flavor content of the final state hadron in current fragmentation (detecting the target hadron)
- study entanglement in correlations in target vs current
- access quark short-range correlations and χSB (Schweitzer et al)
- ...

B2B hadron production in SIDIS: First measurements

M. Anselmino, V. Barone and A. Kotzinian, Physics Letters B 713 (2012)

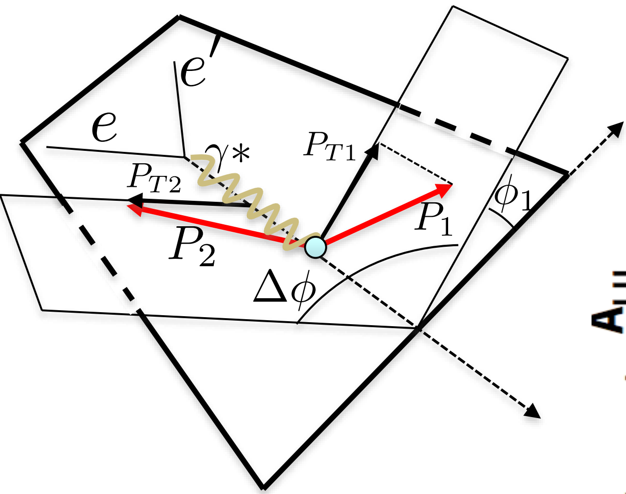

$$A_{LU} = -\frac{y(1-\frac{y}{2})}{(1-y+\frac{y^2}{2})}\frac{\mathcal{F}_{LU}^{\sin\Delta\phi}}{\mathcal{F}_{UU}}\sin\Delta\phi$$

$$= -\frac{|\boldsymbol{P}_{1\perp}||\boldsymbol{P}_{2\perp}|}{m_N m_2}\frac{y(1-\frac{y}{2})}{(1-y+\frac{y^2}{2})}\frac{\mathcal{C}[w_5 M_L^{\perp,h} D_1]}{\mathcal{C}[M D_1]}\sin\Delta\phi.$$

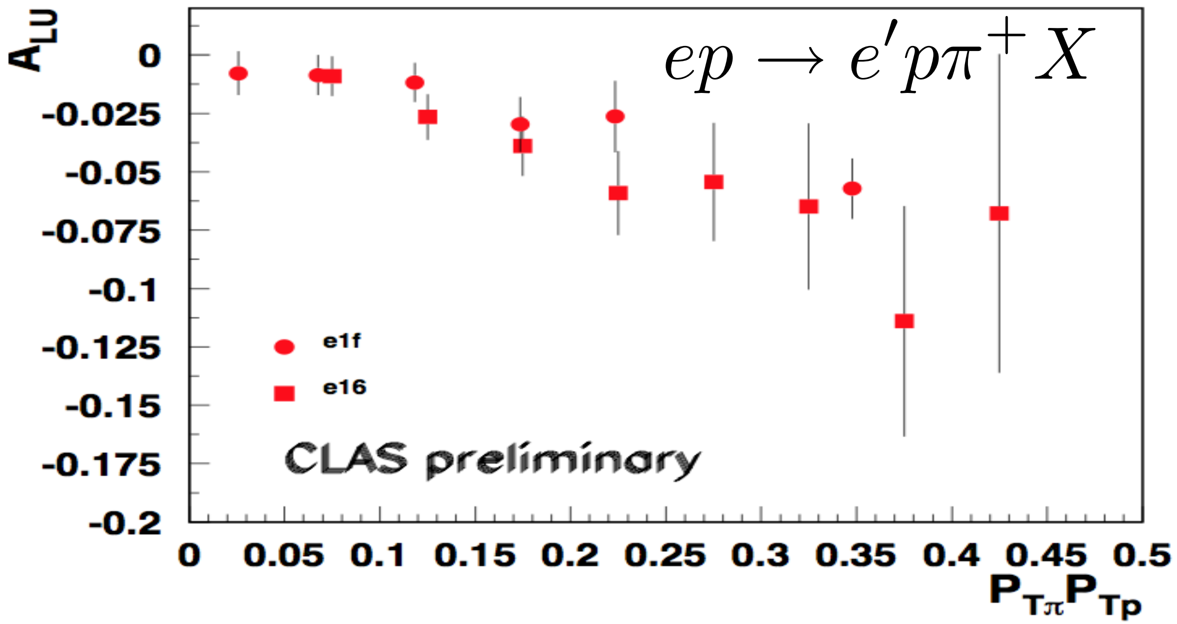

Asymmetry transverse momentum dependence (linear with $P_{T\pi}P_{Tp}$) consistent with theory prediction

Summary

- The $\cos\varphi_h$ and $\cos2\varphi_h$ modulations measured for both charged pion channels in a fully differential way are significant, depend on flavor, and their understanding is important for interpretation of spin-azimuthal asymmetries

- Comparison of azimuthal moments with HERMES, supports the higher twist nature of the $\cos\varphi_h$moment (Cahn effect).

- Single-target and beam-target spin asymmetries have been measured with high precision, indicting suppression for spin effects in π^0 production in DIS

- Spin asymmetries in the back-to-back di-hadron production have been measured for the first time indicating strong correlation between target and current fragmentation regions.

Support slides….

Extraction and VAlidation (EVA) framework for 3D PDFs

TMDlib and TMDplotter version 1.0.0”
Hautman et al Preprint 1408.3015

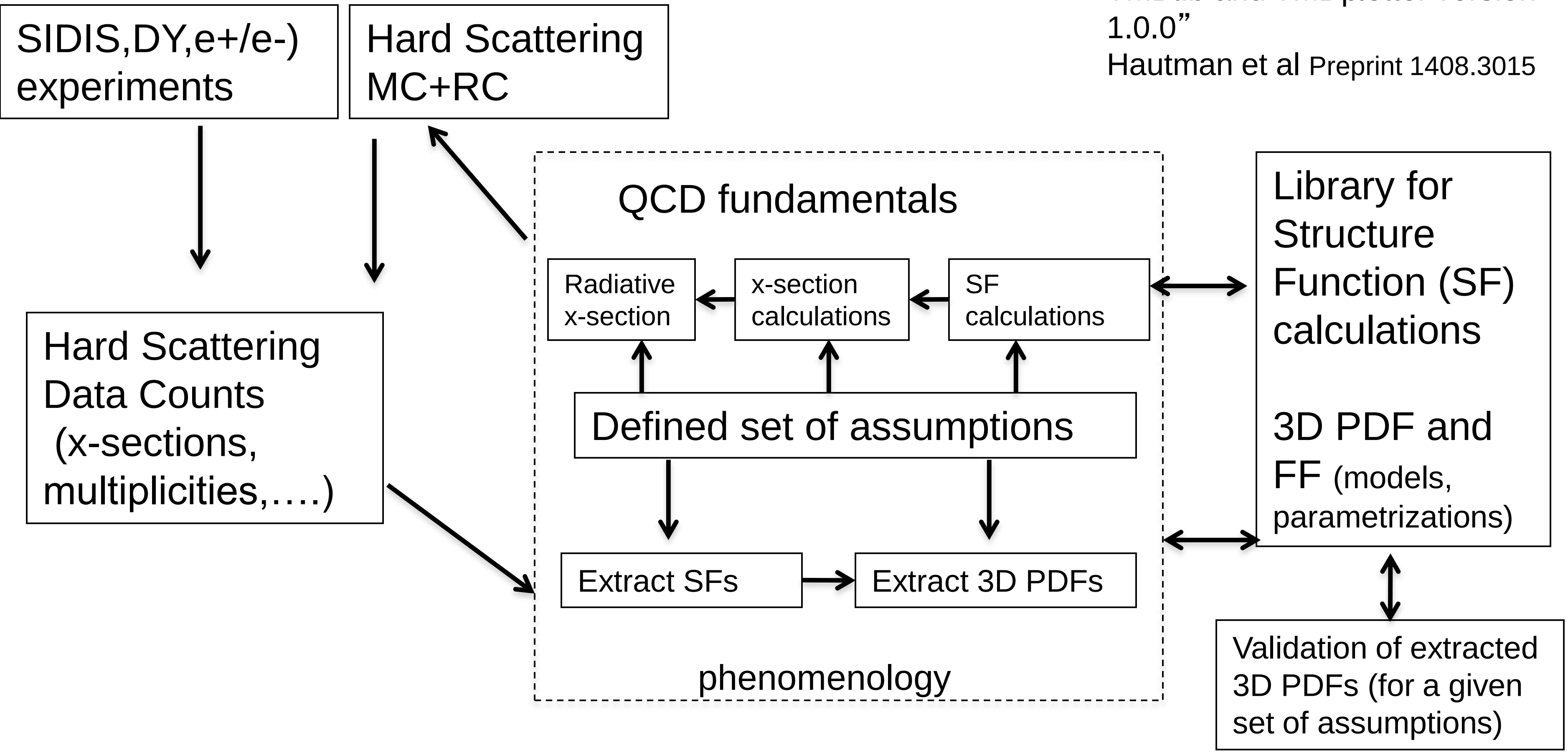

Development of a reliable techniques for the extraction of 3D PDFs and fragmentation functions from the multidimensional experimental observables with controlled systematics requires close collaboration of experiment, theory and computing

Double-Spin Asymmetry (DSA)

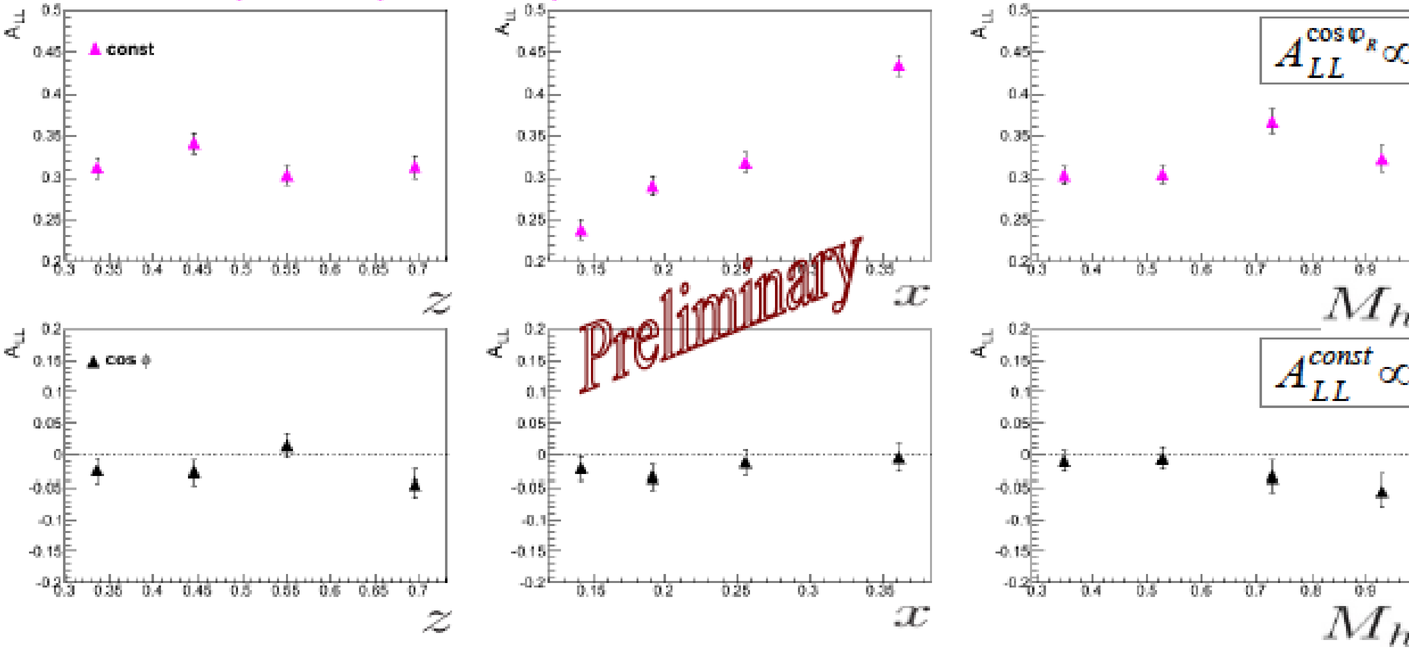

$$A_{LL}^{\cos\varphi_R} \propto g_1(x)\, D^{\sphericalangle q}(z, \cos\theta, M_h)$$

$$A_{LL}^{const} \propto g_1(x)\, D_1^q(z, \cos\theta, M_h)$$

- Significantly non-zero A_{LL}^{const} asymmetries

- We measure

$$A_{LL}^{const} \approx \frac{F_{UU}}{F_{LL}}$$

$$\approx \quad \frac{g_1^q(x)\, D_1^q(z, \cos\theta, M_h)}{f_1^q(x)\, D_1^q(z, \cos\theta, M_h)}$$

- This comparison shows that the present A_{LL}^{const} results are very consistent

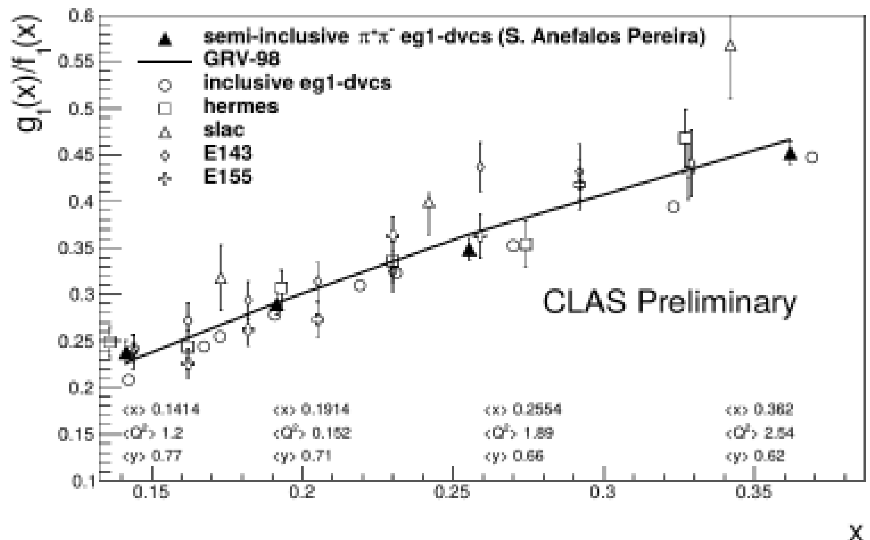

Model predictions for cosϕ

$$F_{UU,T} + \varepsilon F_{UU,L} + \sqrt{2\,\varepsilon(1+\varepsilon)}\,\cos\phi_h\,F_{UU}^{\cos\phi_h}$$

$$F_{UU}^{\cos\phi_h} = \frac{2M}{Q}\,\mathcal{C}\Big[-\frac{\hat{\boldsymbol{h}}\cdot\boldsymbol{k}_T}{M_h}\Big(xh\,H_1^\perp + \frac{M_h}{M}\,f_1\frac{\tilde{D}^\perp}{z}\Big) - \frac{\hat{\boldsymbol{h}}\cdot\boldsymbol{p}_T}{M}\Big(x f^\perp D_1 + \frac{M_h}{M}\,h_1^\perp\frac{\tilde{H}}{z}\Big)\Big]$$

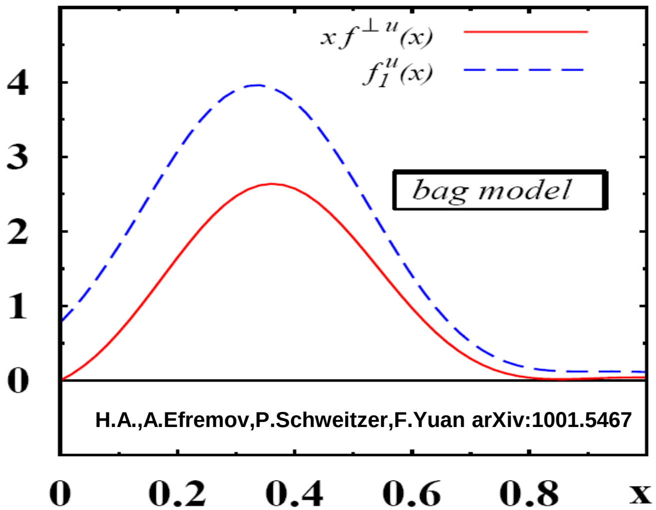

$$F_{UU}^{\cos\phi} \propto f^{\perp q} D_1^q$$

$$x f^{\perp q} = x\tilde{f}^{\perp q} + f_1^q$$

"interaction dependent"

Models agree on a large HT distributions

Extracting the average transverse momenta

V. Barone, M. Boglione, J. O. Gonzalez Hernandez, S. Melis

$$F_{UU}^{\cos\phi}|_{\mathrm{Cahn}} = -2\sum_q e_q^2 x \int d^2\boldsymbol{k}_\perp \frac{(\boldsymbol{k}_\perp \cdot \boldsymbol{h})}{Q} f_q(x, k_\perp) D_q(z, p_\perp), \quad (9)$$

$$\frac{\left(F_{UU}^{\cos\phi_h}\right)_{Cahn}}{F_{UU}} \propto \frac{\langle k_\perp^2 \rangle}{\langle P_T^2 \rangle}$$

$$\langle cos(\phi) \rangle \propto \frac{\left(F_{UU}^{\cos\phi_h}\right)_{Cahn}}{F_{UU}} + \frac{\left(F_{UU}^{\cos\phi_h}\right)_{BM}}{F_{UU}}$$

$$F_{UU}^{\cos\phi}|_{\mathrm{BM}} = \sum_q e_q^2 x \int d^2\boldsymbol{k}_\perp \frac{k_\perp}{Q} \frac{P_T - z(\boldsymbol{k}_\perp \cdot \boldsymbol{h})}{p_\perp} \times \Delta f_{q^\uparrow/p}(x, k_\perp) \Delta D_{h/q^\uparrow}(z, p_\perp). \quad (10)$$

$$\Delta f_{q^\uparrow/p}(x, k_\perp) = \Delta f_{q^\uparrow/p}(x) \sqrt{2e} \frac{k_\perp}{M_{\mathrm{BM}}} \frac{e^{-k_\perp^2/\langle k_\perp^2 \rangle_{\mathrm{BM}}}}{\pi \langle k_\perp^2 \rangle}$$

$$F_{UU} = \sum_q e_q^2 x_B f_{q/p}(x_B) D_{h/q}(z_h) \frac{e^{-P_T^2/\langle P_T^2 \rangle}}{\pi \langle P_T^2 \rangle},$$

$$F_{UU}^{\cos\phi}|_{\mathrm{Cahn}} = -2\frac{P_T}{Q} \sum_q e_q^2 x_B f_{q/p}(x_B) D_{h/q}(z_h) \frac{z_h \langle k_\perp^2 \rangle}{\langle P_T^2 \rangle} \frac{e^{-P_T^2/\langle P_T^2 \rangle}}{\pi \langle P_T^2 \rangle},$$

$$F_{UU}^{\cos\phi}|_{\mathrm{BM}} = 2e \frac{P_T}{Q} \sum_q e_q^2 x_B \frac{\Delta f_{q^\uparrow/p}(x_B)}{M_{\mathrm{BM}}} \frac{\Delta D_{h/q^\uparrow}(z_h)}{M_C} \frac{e^{-P_T^2/\langle P_T^2 \rangle_{\mathrm{BM}}}}{\pi \langle P_T^2 \rangle_{\mathrm{BM}}^4} \times \frac{\langle k_\perp^2 \rangle_{\mathrm{BM}}^2 \langle p_\perp^2 \rangle_C^2}{\langle k_\perp^2 \rangle \langle p_\perp^2 \rangle} [z_h^2 \langle k_\perp^2 \rangle_{\mathrm{BM}} (P_T^2 - \langle P_T^2 \rangle_{\mathrm{BM}}) + \langle p_\perp^2 \rangle_C \langle P_T^2 \rangle_{\mathrm{BM}}],$$

cos ϕ has much greater sensitivity to $<k_T>$

φ_h distributions - raw data (lowest x-Q^2 bin)

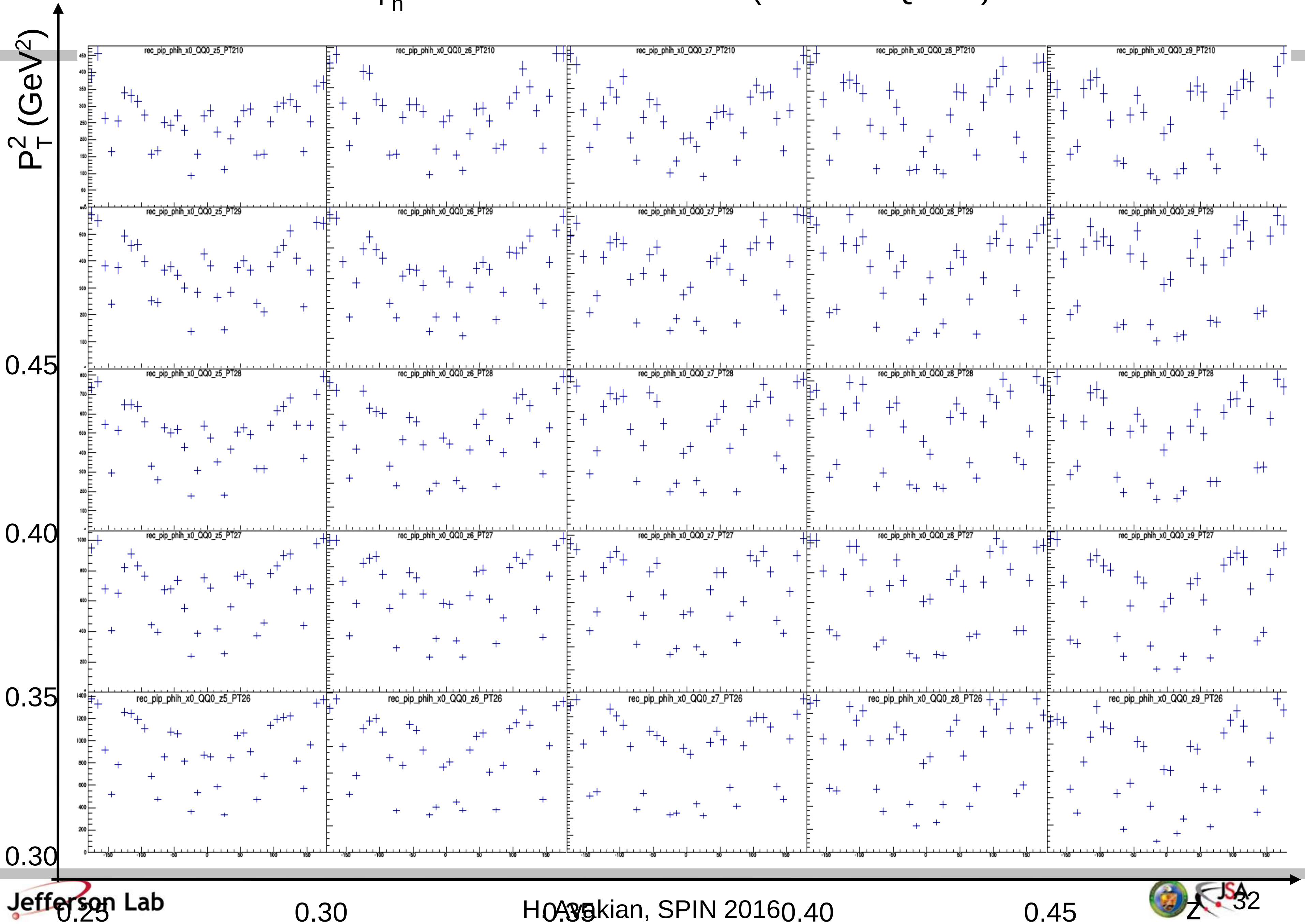

Example of a EBC table

N. Harrison
(e1f:CLAS@5.5)

5D tables (counts in bins of x, Q^2, z, PT^2, \phi_h):

column 1: x bin number (0-4)
column 2: Q^2 bin number (0-1)
column 3: z bin number (0-17)
column 4: PT^2 bin number (0-19)
column 5: phi bin number (0-35)
column 6: <x>
column 7: <Q^2> (GeV^2)
column 8: <z>
column 9: <PT^2> (GeV^2)
column 10: <phi> (degrees)

column 11: <y>
column 12: number of counts, corrected for acceptance and radiative effects
column 13: statistical error on the the number of counts
column 14: the radiative correction factor

0	0	2	3	19	0.147459	1.16316	0.126884	0.171938	15	0.770322	20528	472.849	1.06035
0	0	2	3	20	0.147459	1.16316	0.126884	0.171938	25	0.770322	19958.1	619.905	1.06123
0	0	2	3	21	0.147459	1.16316	0.126884	0.171938	35	0.770322	20775.6	541.396	1.06257
0	0	2	3	22	0.147459	1.16316	0.126884	0.171938	45	0.770322	19948.5	434.023	1.06435
0	0	2	3	23	0.147459	1.16316	0.126884	0.171938	55	0.770322	21764.5	465.939	1.06671
0	0	2	3	24	0.147459	1.16316	0.126884	0.171938	65	0.770322	20436.3	445.162	1.06951
0	0	2	3	25	0.147459	1.16316	0.126884	0.171938	75	0.770322	20714.1	495.978	1.07289
0	0	2	3	26	0.147459	1.16316	0.126884	0.171938	85	0.770322	20714.4	634.193	1.07689
0	0	2	3	27	0.147459	1.16316	0.126884	0.171938	95	0.770322	21371.5	523.387	1.08116
0	0	2	3	28	0.147459	1.16316	0.126884	0.171938	105	0.770322	21770.1	460.747	1.08614
0	0	2	3	29	0.147459	1.16316	0.126884	0.171938	115	0.770322	21471.5	452.809	1.09134
0	0	2	3	30	0.147459	1.16316	0.126884	0.171938	125	0.770322	22028.4	467.693	1.09713
0	0	2	3	31	0.147459	1.16316	0.126884	0.171938	135	0.770322	24086.5	536.874	1.10245
0	0	2	3	32	0.147459	1.16316	0.126884	0.171938	145	0.770322	21488.1	616.541	1.10712
0	0	2	3	33	0.147459	1.16316	0.126884	0.171938	155	0.770322	23926.8	605.209	1.11166

Representative Results

A_0 (top row), $A_{UU}^{\cos\phi_h}$ (middle row), and $A_{UU}^{\cos 2\phi_h}$ (bottom row) vs P_T^2 for π+ and π-

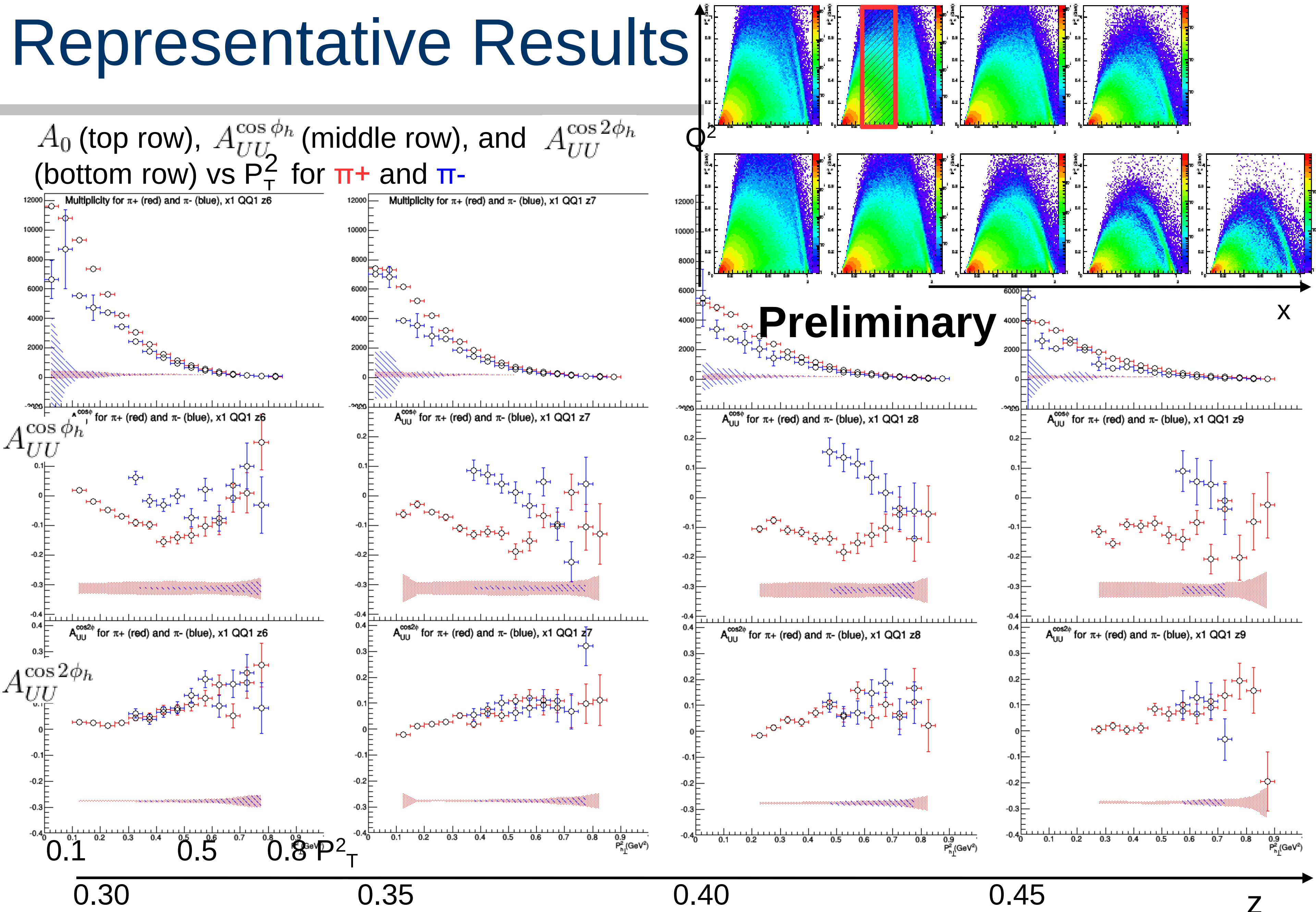

(high Q^2 bin of 0.2 < x < 0.3)

Representative Results

A_0 (top row), $A_{UU}^{\cos\phi_h}$ (middle row), and $A_{UU}^{\cos 2\phi_h}$ (bottom row) vs P_T^2 for π+ and π-

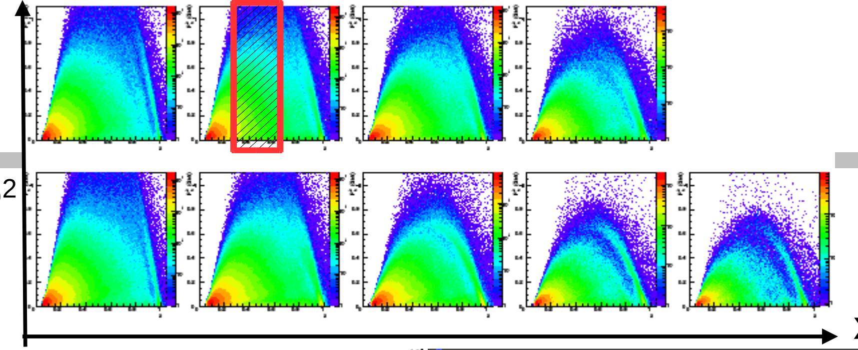

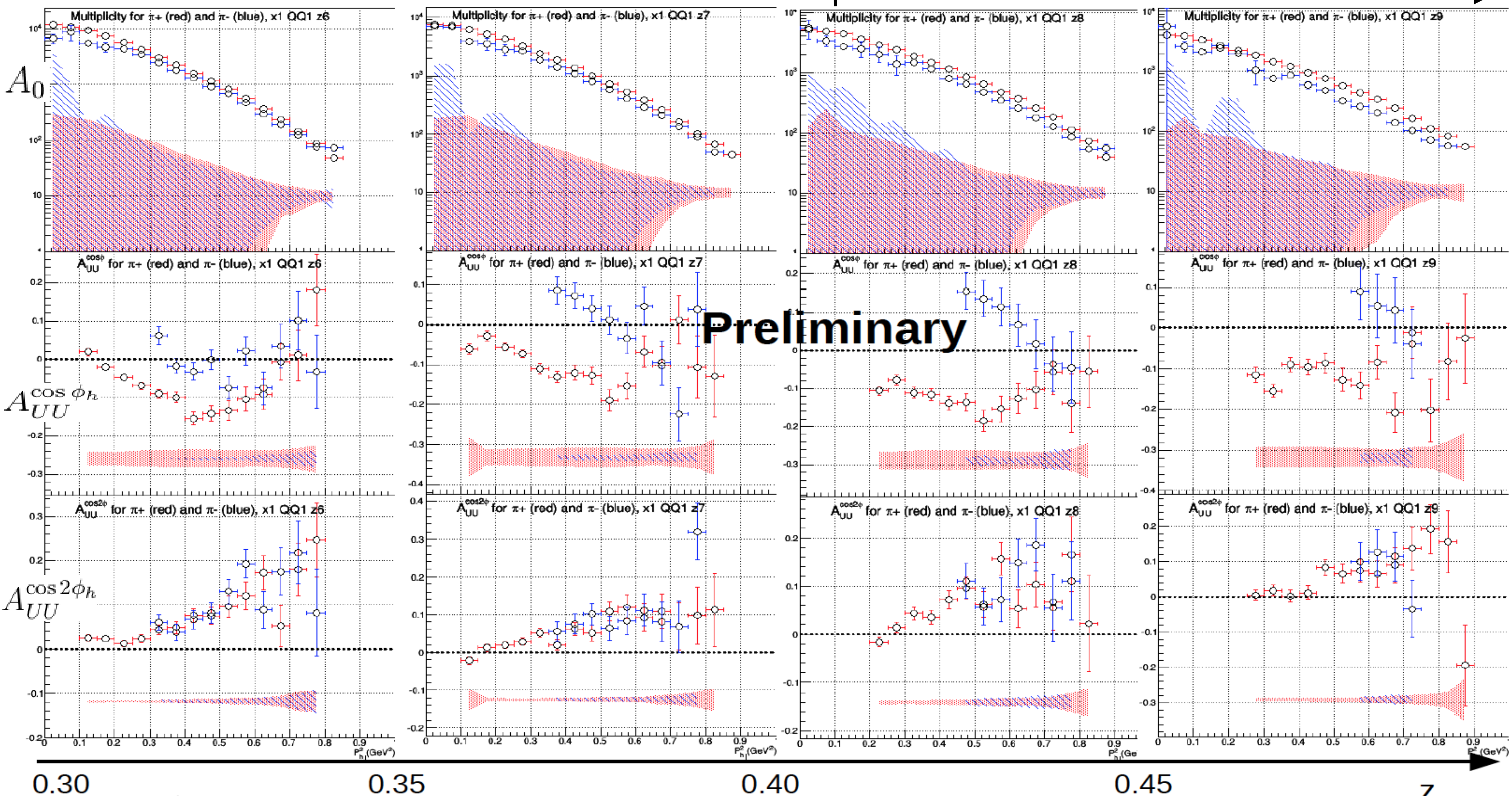

(high Q^2 bin of $0.2 < x < 0.3$)

Radiative Corrections

- Radiative effects, such as the emission of a photon by the incoming or outgoing electron, can change all five SIDIS kinematic variables.

- Furthermore, exclusive events can enter into the SIDIS sample because of radiative effects ("exclusive tail").

- HAPRAD 2.0 is used to do radiative corrections.

- For a given $\sigma_{Born}\left(x, Q^2, z, P_{h\perp}^2, \phi_h\right)$ (obtained from a model), HAPRAD calculates $\sigma_{rad+tail}\left(x, Q^2, z, P_{h\perp}^2, \phi_h\right)$. The correction factor is then:

$$RC\ factor = \frac{\sigma_{rad+tail}\left(x, Q^2, z, P_{h\perp}^2, \phi_h\right)}{\sigma_{Born}\left(x, Q^2, z, P_{h\perp}^2, \phi_h\right)}$$

- 3 different models were used to study model dependence.

Monte Carlo φ generated, reconstructed, and acceptance for π+ (lowest x-Q^2 bin)

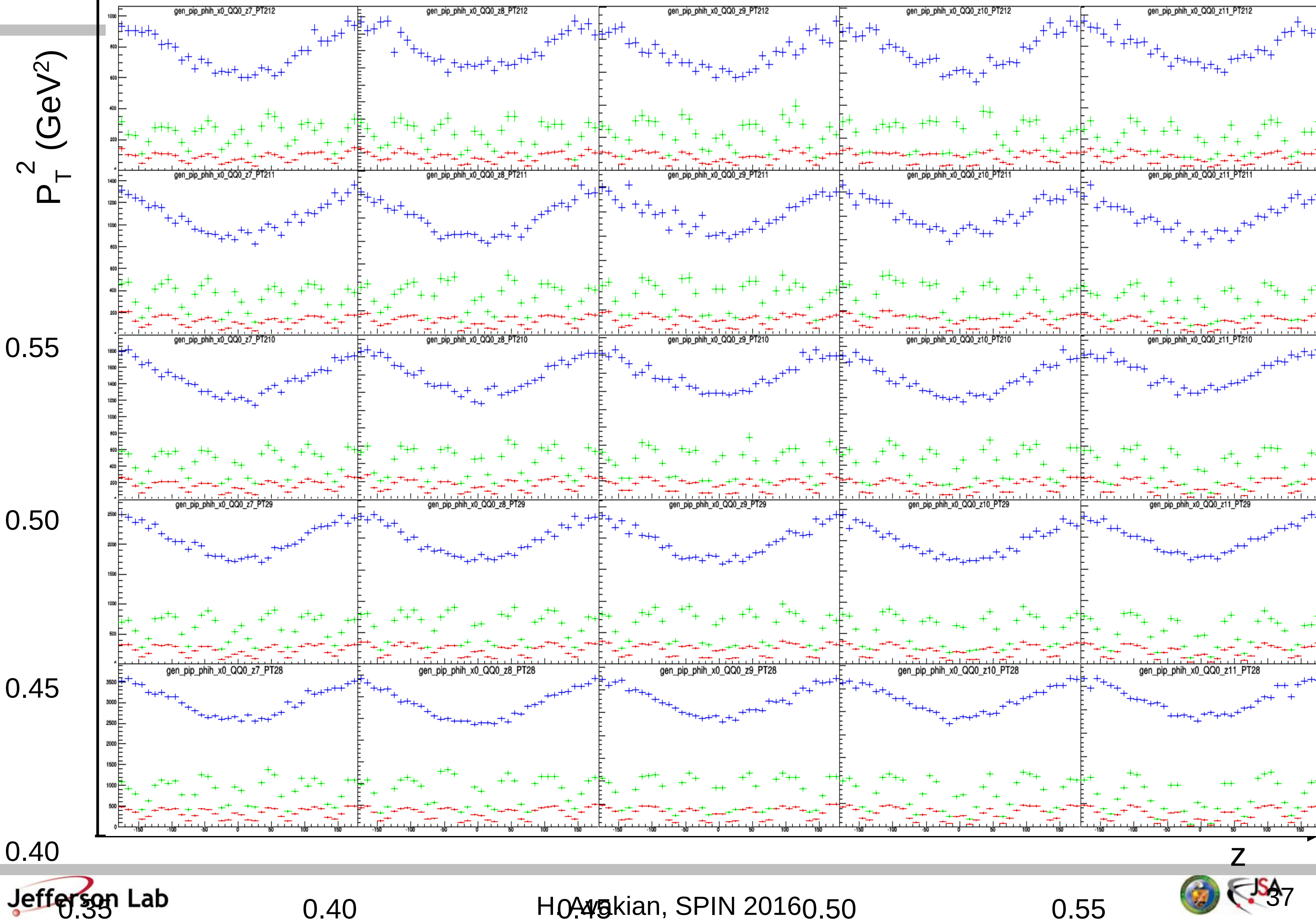

Born, radiated, and exclusive tail cross-sections from HAPRAD (lowest x-Q^2 bin)

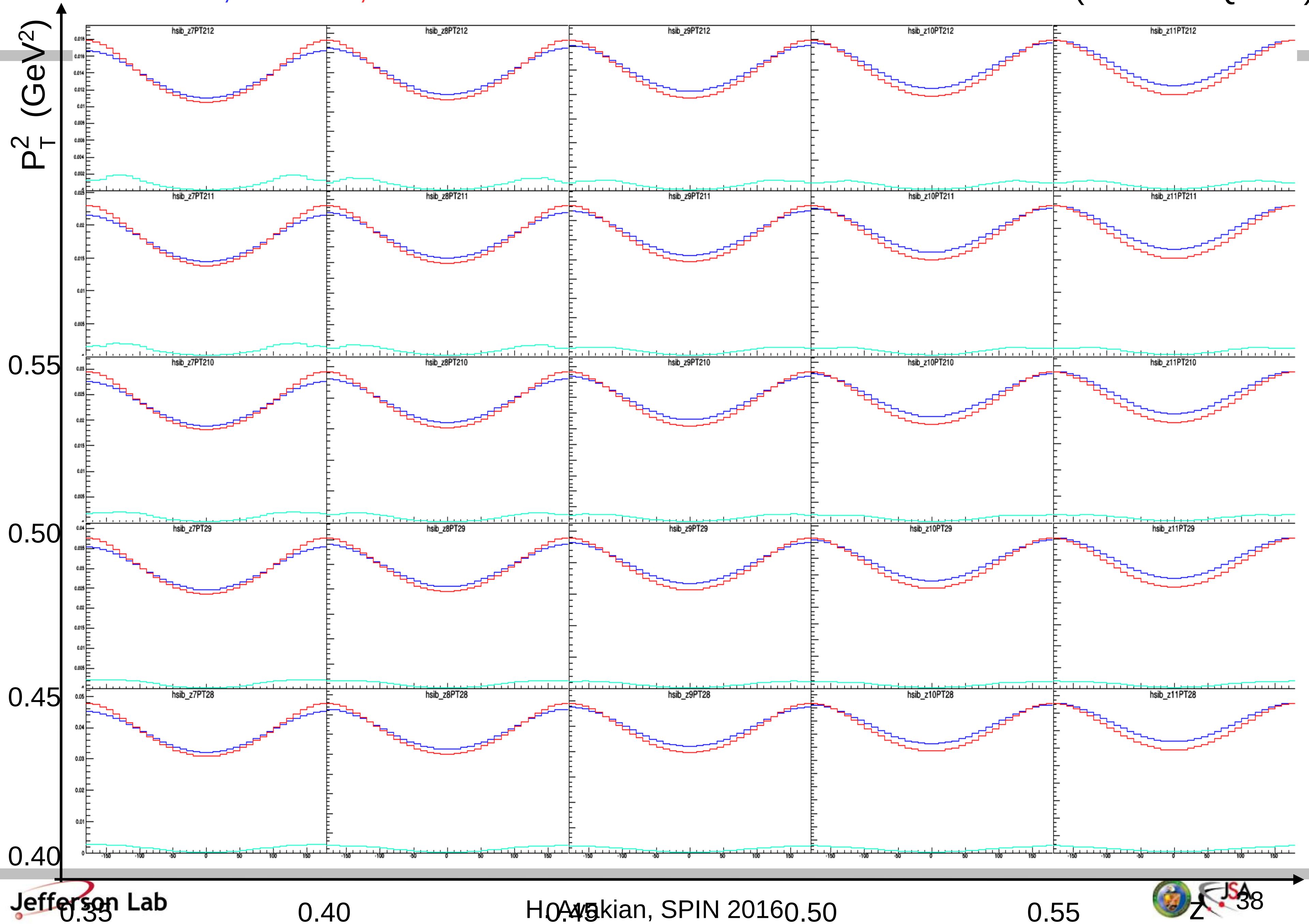

SIDIS asymmetries from eg1-dvcs data

- eg1-dvcs vs theory

Nuclear Physics A 941 (2015) 307–334

The Bourrely & Soffer quantum statistical parton distribution model incorporates physical principles to reduce the number of free parameters which have a physical interpretation.

ii) It has very specific predictions, so far confirmed by the data.
iii) It is an attempt to reach a more physical picture on our knowledge of the nucleon structure, the ultimate goal would be to solve the problem of confinement.
iv) Treating simultaneously unpolarized distributions and helicity distributions, a unique situation in the literature, has the advantage to give access to a vast set of experimental data, in particular up to LHC energies

In literature, different choices have been made for the propagator of the vector diquark $d_{\mu\nu}$. As shown in Ref. [37], different forms of $d_{\mu\nu}$ generally lead to different results of the correlator. The spectator model including a correct polarization sum was studied in Ref. [43]. In this work, we will consider two choices for $d_{\mu\nu}$ for comparison. The first one has the form:

$$d^{\mu\nu}(k) = -g^{\mu\nu} + \frac{k^\mu n_-^\nu + k^\nu n_-^\mu}{k \cdot n_-} - \frac{M_v^2}{[k \cdot n_-]^2} n_-^\mu n_-^\nu, \tag{20}$$

which is motivated by the light-cone formalism [32] for the vector diquarks. Applying the propagator (20), we obtain the corresponding contributions to $g_L^\perp$ and e_L from the axial-vector diquark component:

$$g_L^{\perp v}(x, \boldsymbol{k}_T^2)\big|_{\text{Set I}} = \frac{N_v^2(1-x)}{16\pi^3} \frac{(1-x)\left[(m+xM)^2 + (1-x)M^2\right] - M_v^2 + x\boldsymbol{k}_T^2}{(\boldsymbol{k}_T^2 + L_v^2)^4}, \tag{21}$$

$$e_L^v(x, \boldsymbol{k}_T^2)\big|_{\text{Set I}} = 0, \tag{22}$$

and we denote them as the Set I results of f^v.

The second form for the vector diquark propagator employed in our calculation is

$$d^{\mu\nu}(k) = -g^{\mu\nu}, \tag{23}$$

which has been applied in Ref. [35]. Similarly, using (23) we obtain alternative expressions for $g_L^{\perp v}$ and e_L^v:

$$g_L^{\perp v}(x, \boldsymbol{k}_T^2)\Big|_{\text{Set II}} = \frac{N_v^2(1-x)^2}{16\pi^3} \frac{(1-x)^2M^2 - M_v^2 - \boldsymbol{k}_T^2}{(\boldsymbol{k}_T^2 + L_v^2)^4}, \tag{24}$$

$$e_L^v(x, \boldsymbol{k}_T^2)\Big|_{\text{Set II}} = C_F\alpha_s \frac{{N_v}^2(1-x)^2}{32\pi^3} \frac{(x + \frac{m}{M})(L_v^2 - \boldsymbol{k}_T^2)}{L_v^2(L_v^2 + \boldsymbol{k}_T^2)^3}, \tag{25}$$

which we denote as Set II results. Although in our calculations we adopt two polarization sums

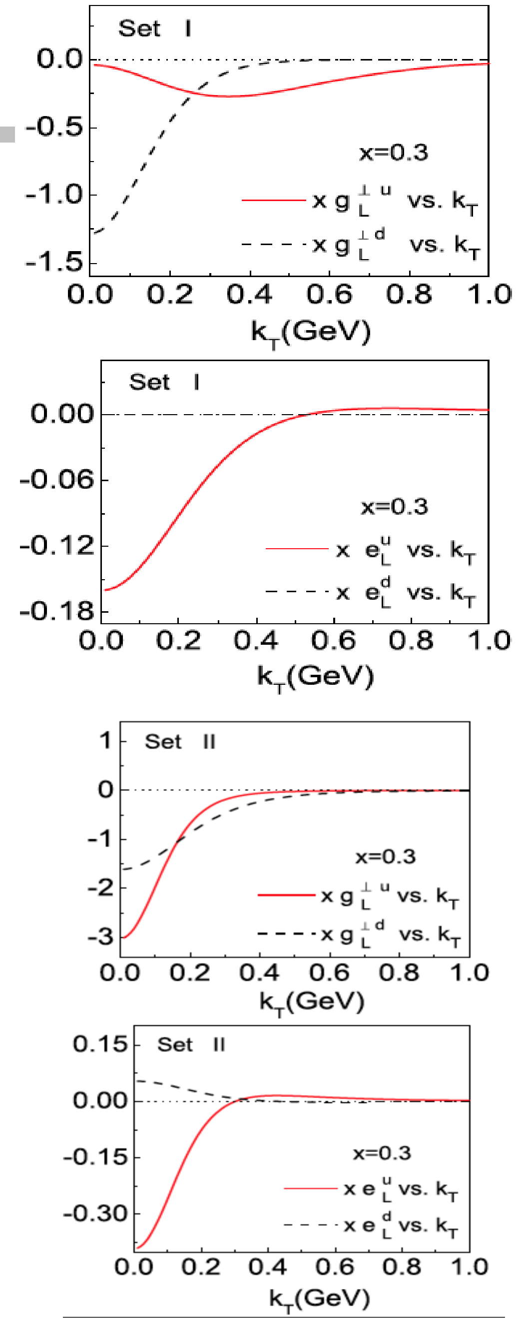

Double spin asymmetry vs x

$$A_{\parallel} \approx \frac{(1-\varepsilon)(2-y)}{y\,(1+\varepsilon R)}\,\frac{g_1}{F_1} \equiv \frac{y(2-y)}{y^2+2\left(1-y-\frac{y^2\gamma^2}{4}\right)\frac{(1+R)}{(1+\gamma^2)}}\frac{g_1}{F_1} \equiv D'(y)\frac{g_1}{F_1}$$

$$\frac{g_1}{F_1} \approx \frac{1}{1+\gamma^2 y/2} A_1$$

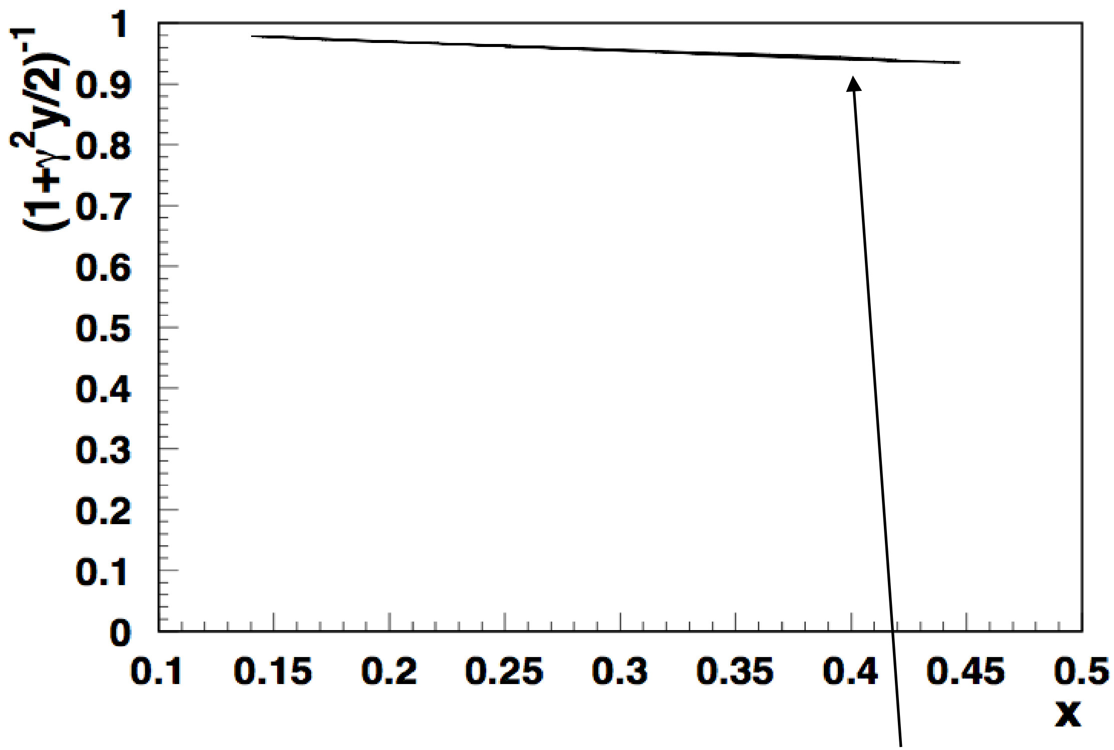

At large x the difference between A_1 and $A_{\parallel}$ becomes more significant(eg1dvcs kinematic bins).

$A_{LL}^{\cos\phi}$: First measurement & possible interpretation

N/q	U	L	T
U	$f^\perp$	$g^\perp$	$h, \mathbf{e}$
L	$f_L^\perp$	$g_L^\perp$	$\mathbf{h_L}, e_L$
T	$f_T, f_T^\perp$	$\mathbf{g_T}, g_T^\perp$	$h_T, e_T, h_T^\perp, e_T^\perp$

q/h	U	L	T
U	$\mathbf{D_1}$		$D_{1T}^\perp$
L		$\mathbf{G_{1L}}$	$G_{1T}^\perp$
T	$H_1^\perp$	$H_{1L}^\perp$	$\mathbf{H_1}$ $H_{1T}^\perp$

$$A_{LL}^{\cos\phi} \propto g_L^\perp D_1 + e_L H_1^\perp$$

W.Mao et al, Nucl.Phys. A945 (2016) 153-167

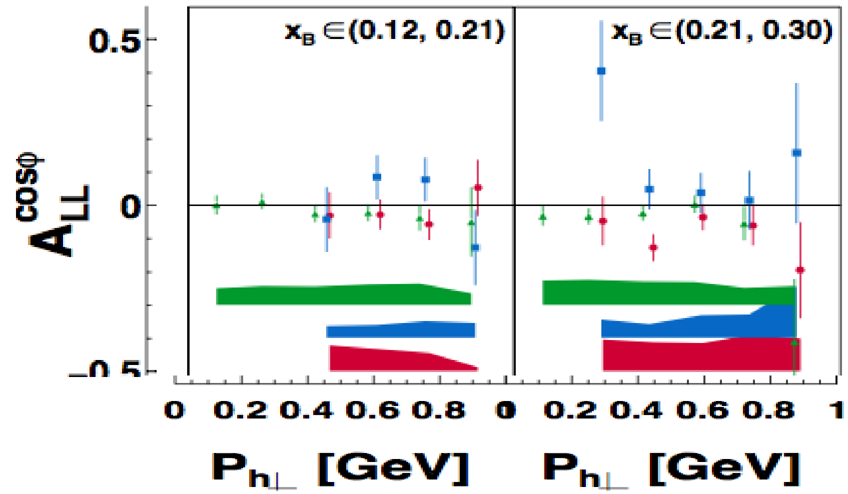

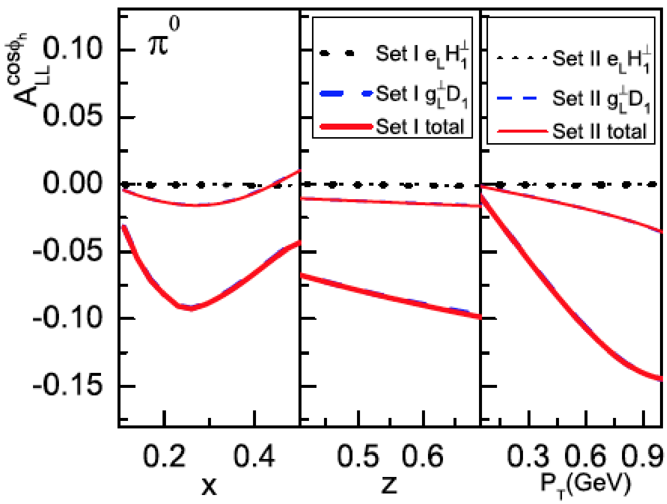

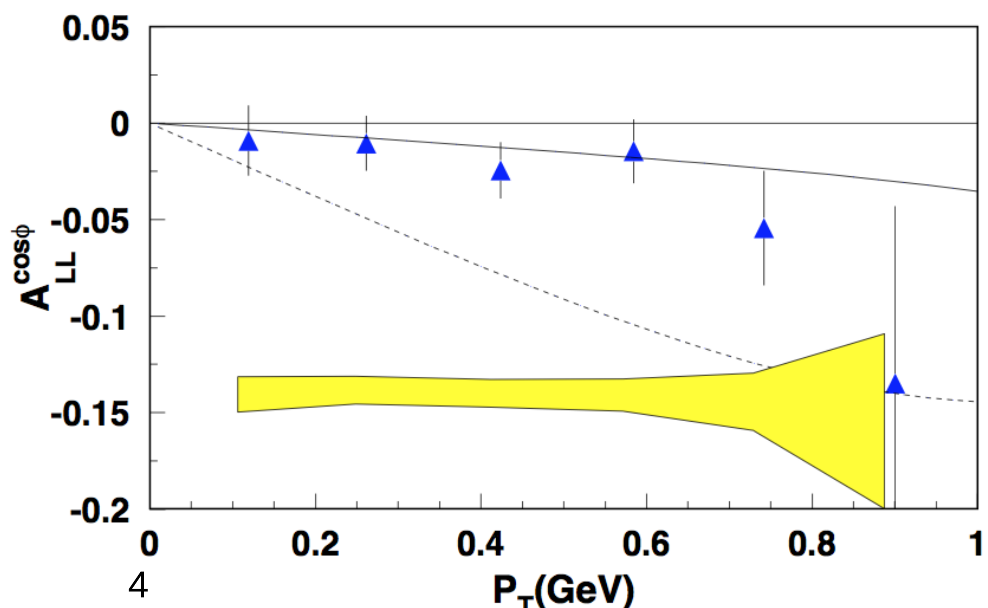

4
2

$A_{UL}^{\sin\phi}$: From measurements to interpretation

N/q	U	L	T
U	$f^{\perp}$	$g^{\perp}$	$h, \mathbf{e}$
L	$f_L^{\perp}$	$g_L^{\perp}$	$\mathbf{h_L}, e_L$
T	$f_T, f_T^{\perp}$	$\mathbf{g_T}, g_T^{\perp}$	$h_T, e_T, h_T^{\perp}, e_T^{\perp}$

q/h	U	L	T
U	$\mathbf{D_1}$		$D_{1T}^{\perp}$
L		$\mathbf{G_{1L}}$	$G_{1T}^{\perp}$
T	$H_1^{\perp}$	$H_{1L}^{\perp}$	$\mathbf{H_1}$ $H_{1T}^{\perp}$

$$A_{UL}^{\sin\phi} \propto f_L^{\perp} D_1 + h_L H_1^{\perp}$$

A.Bacchetta et al, Phys.Rev. D78 (2008) 074010

W. Mao & Z.Lu Eur.Phys.J. C73 (2013) 2557

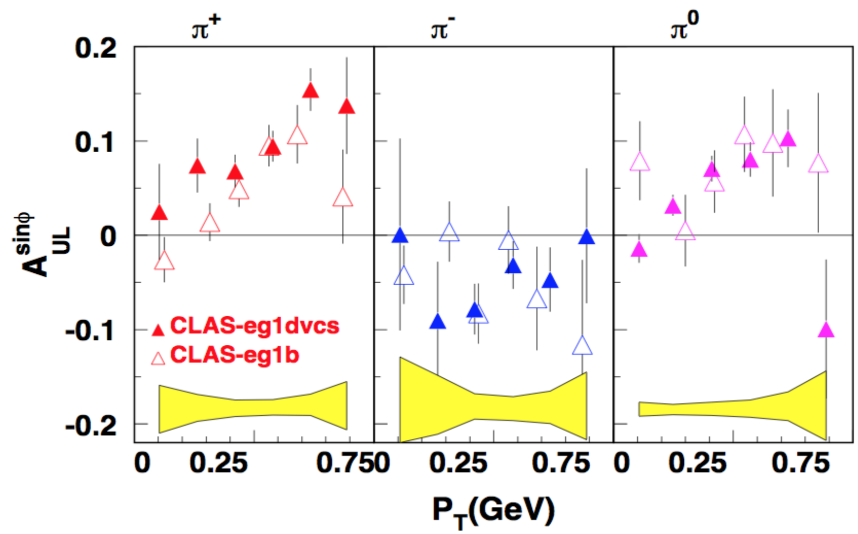

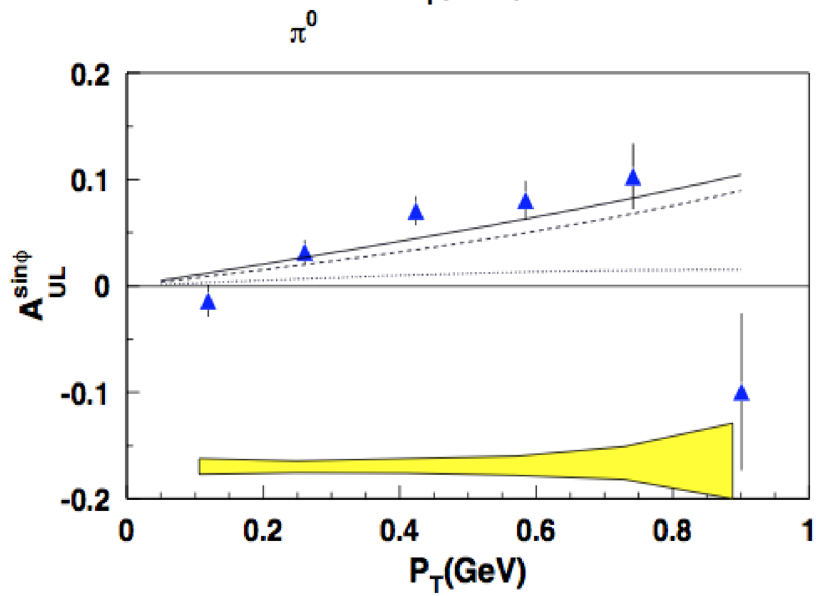

A_{LU} comparing CLAS data sets e16 and e1f

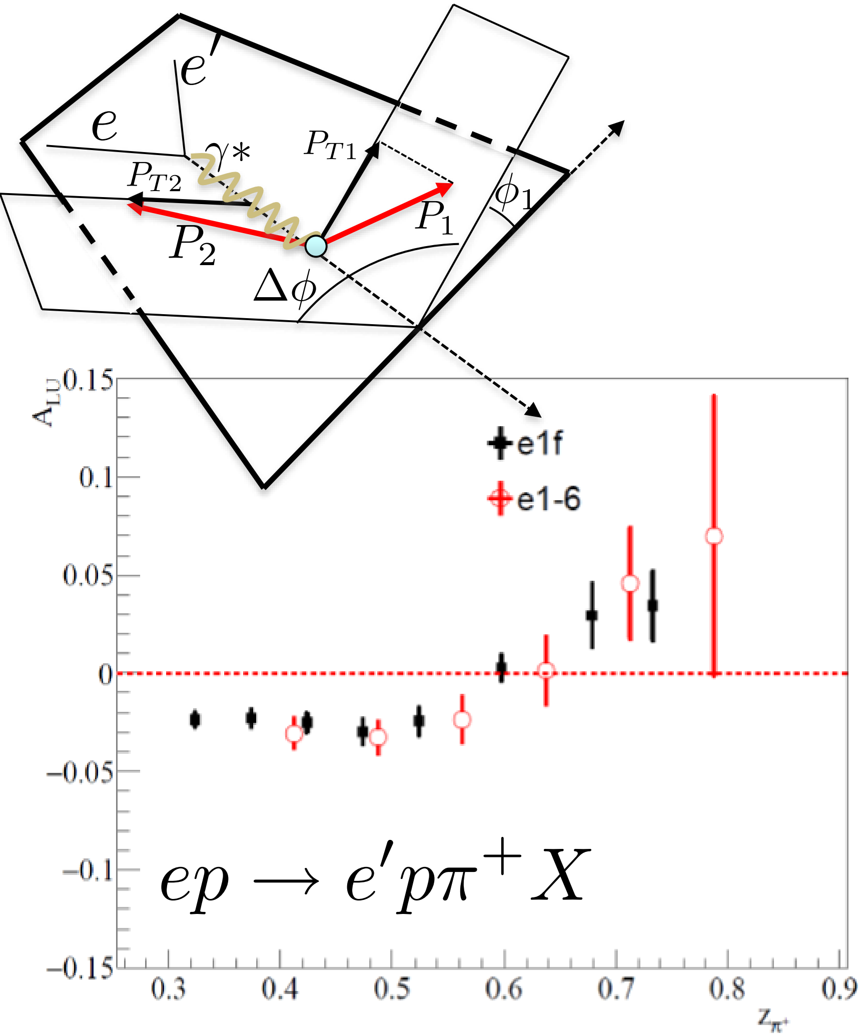

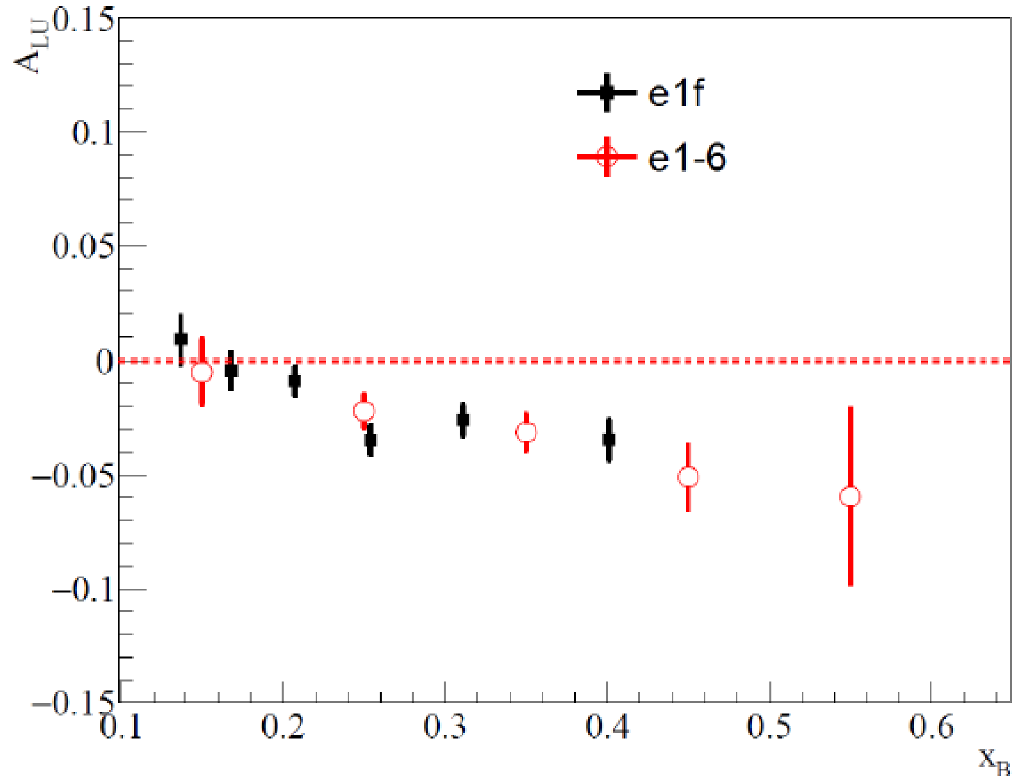

e1f: weaker field, lower Q^2 and x

e16: higher field, higher average Q^2

- Asymmetries may change the sign in the exclusive limit
- Asymmetries are large in the large x-region

π^+ $P^2_{h\perp}$ vs z for each x-Q^2 bin

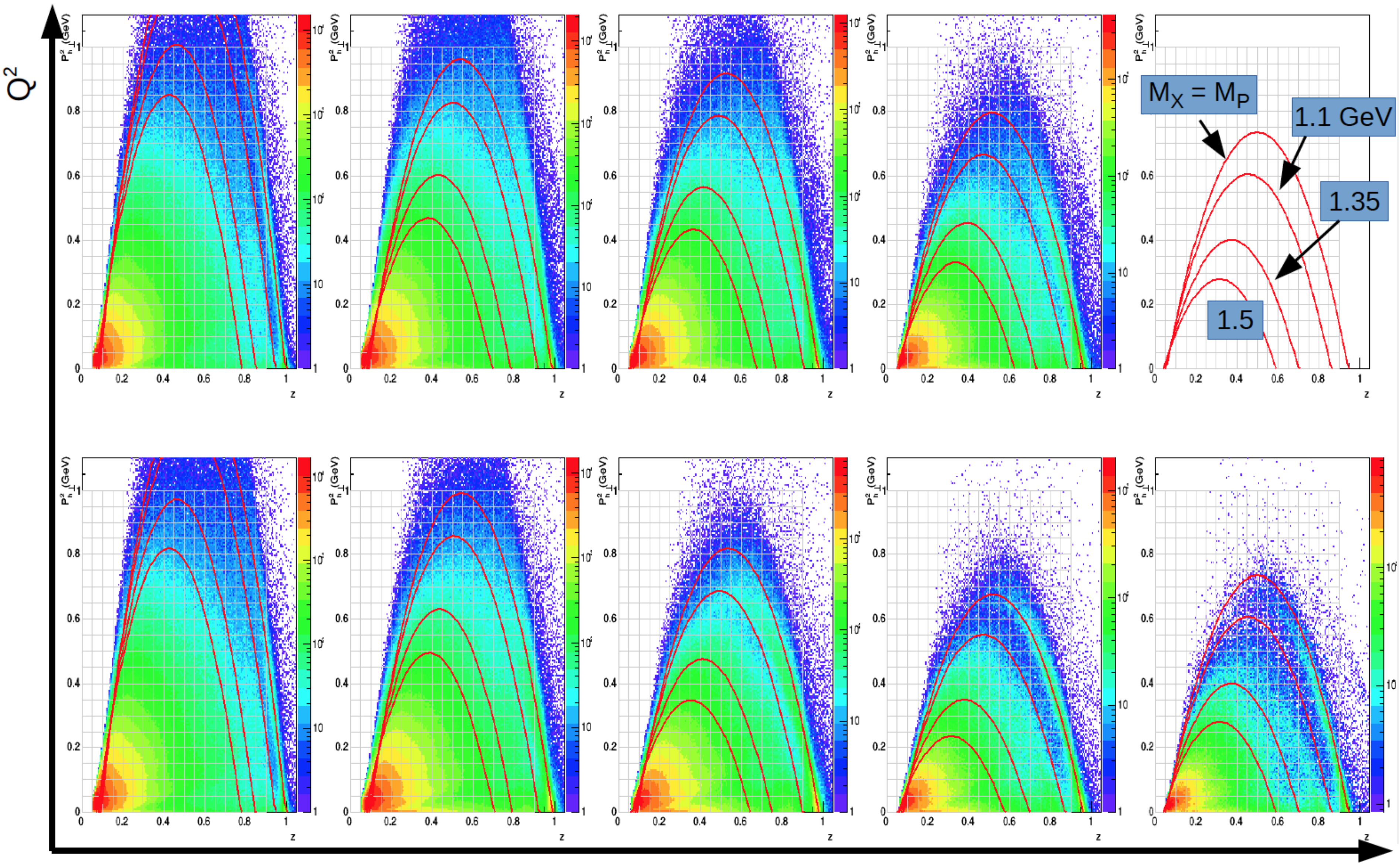

Effects of the shape of the generated ϕ distribution

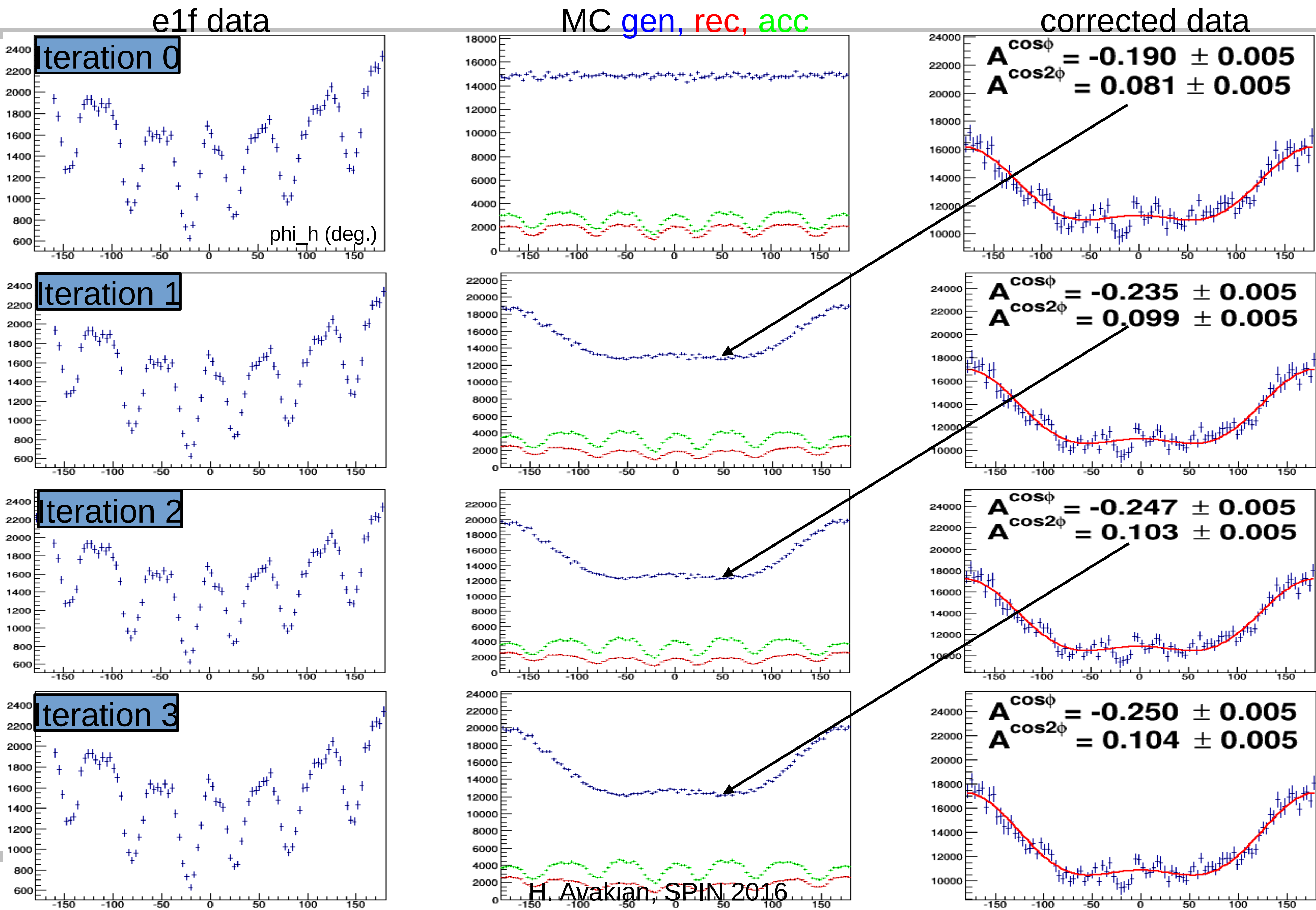

H. Avakian, SPIN 2016

$A_{UU}^{\cos\phi}$: From measurements to interpretation

N/q	U	L	T
U	$f^\perp$	$g^\perp$	$h, \mathbf{e}$
L	$f_L^\perp$	$g_L^\perp$	$\mathbf{h_L}, e_L$
T	$f_T, f_T^\perp$	$\mathbf{g_T}, g_T^\perp$	$h_T, e_T, h_T^\perp, e_T^\perp$

q/h	U	L	
U	$\mathbf{D_1}$		
L		$\mathbf{G_{1L}}$	
T	$H_1^\perp$	$H_{1L}^\perp$	$\mathbf{H}$

$$A_{UU}^{\cos\phi} \propto f^\perp D_1 + hH_1^\perp$$

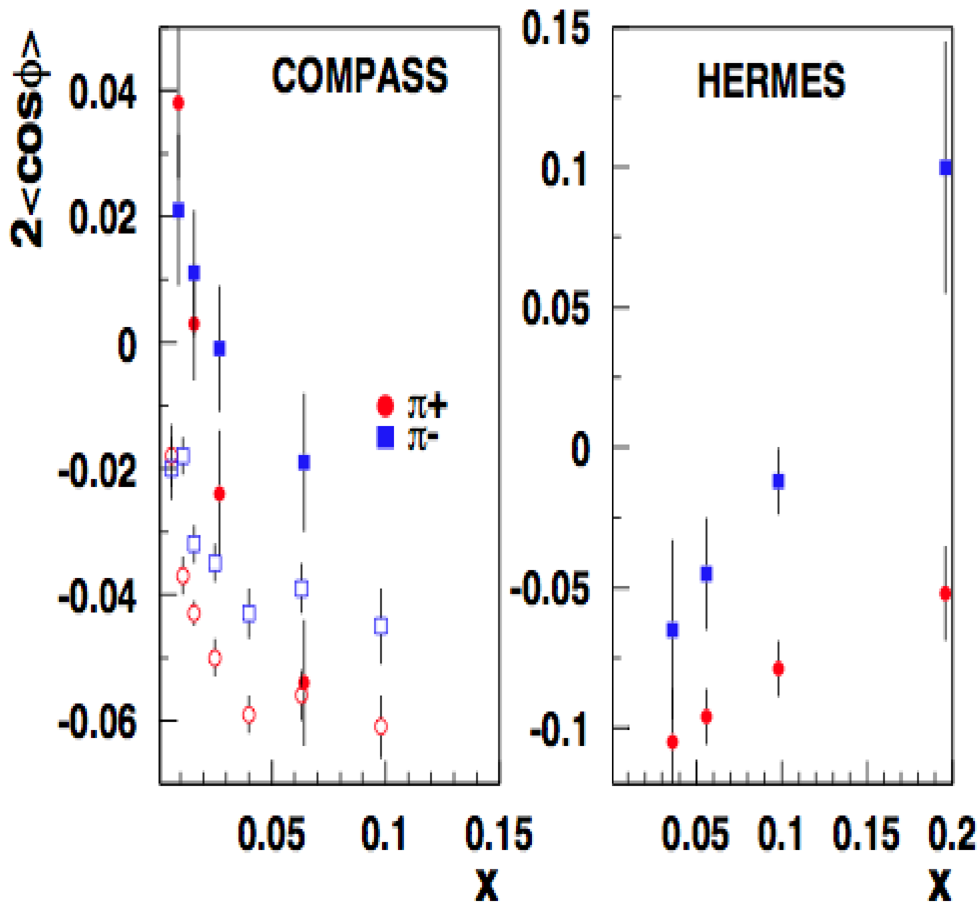

π^0 SSA less sensitive polarized fragmentation effects (Collins function suppressed)

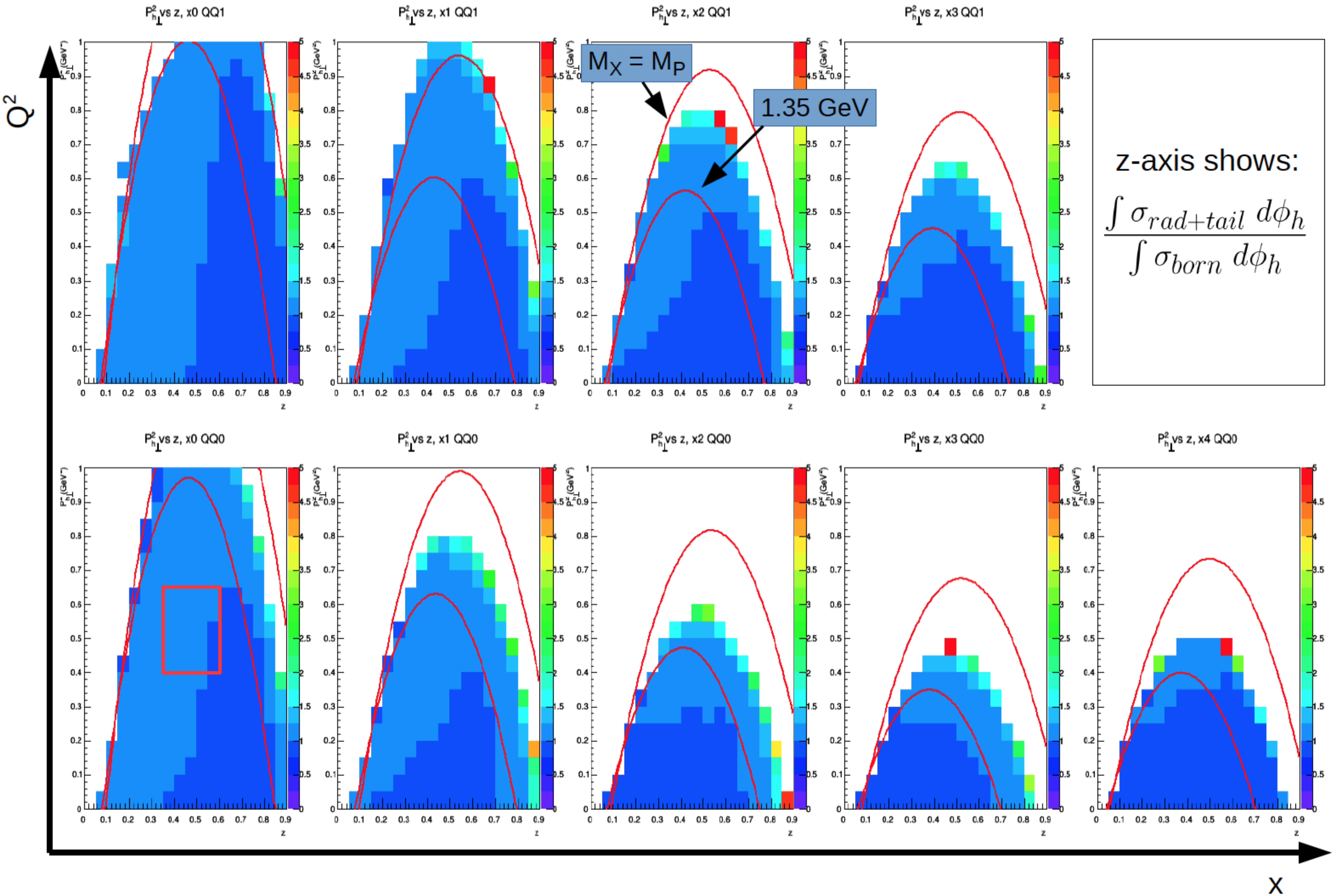

z-axis shows:

$$\frac{\int \sigma_{rad+tail}\, d\phi_h}{\int \sigma_{born}\, d\phi_h}$$

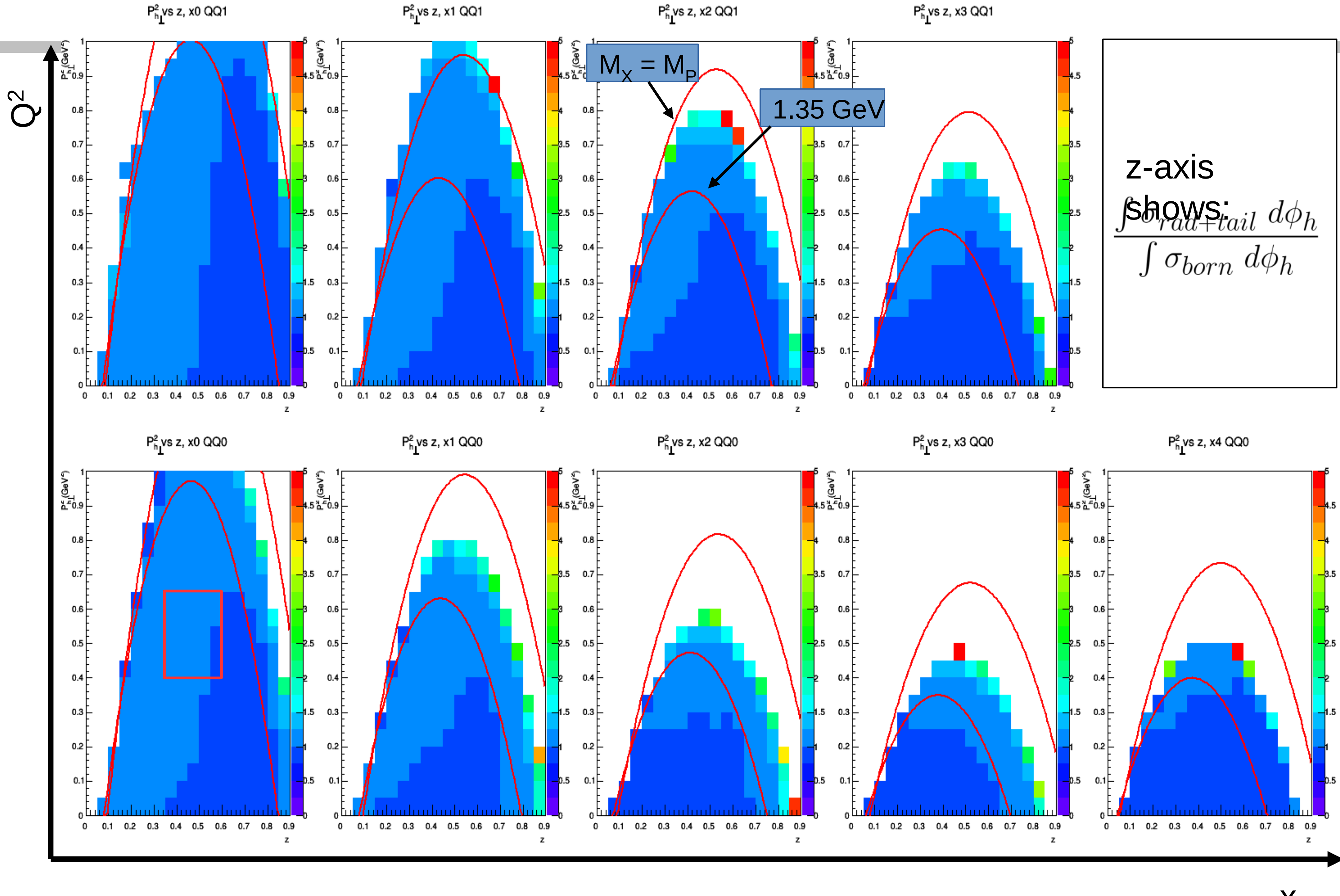

z-axis shows:

$$\frac{\int \sigma_{rad+tail}\, d\phi_h}{\int \sigma_{born}\, d\phi_h}$$

$A_{UL}^{\sin\phi}$:   From measurements to interpretation

N/q	U	L	T
U	$f^{\perp}$	$g^{\perp}$	h, $\mathbf{e}$
L	$f_L^{\perp}$	$g_L^{\perp}$	$\mathbf{h_L}$, e_L
T	$f_T, f_T^{\perp}$	$\mathbf{g_T}, g_T^{\perp}$	$h_T, e_T, h_T^{\perp}, e_T^{\perp}$

q/h	U	L	T
U	$\mathbf{D_1}$		$D_{1T}^{\perp}$
L		$\mathbf{G_{1L}}$	$G_{1T}^{\perp}$
T	$H_1^{\perp}$	$H_{1L}^{\perp}$	$\mathbf{H_1}$ $H_{1T}^{\perp}$

$$A_{UL}^{\sin\phi} \propto f_L^{\perp} D_1 + h_L H_1^{\perp}$$

A.Bacchetta et al, Phys.Rev. D78 (2008) 074010

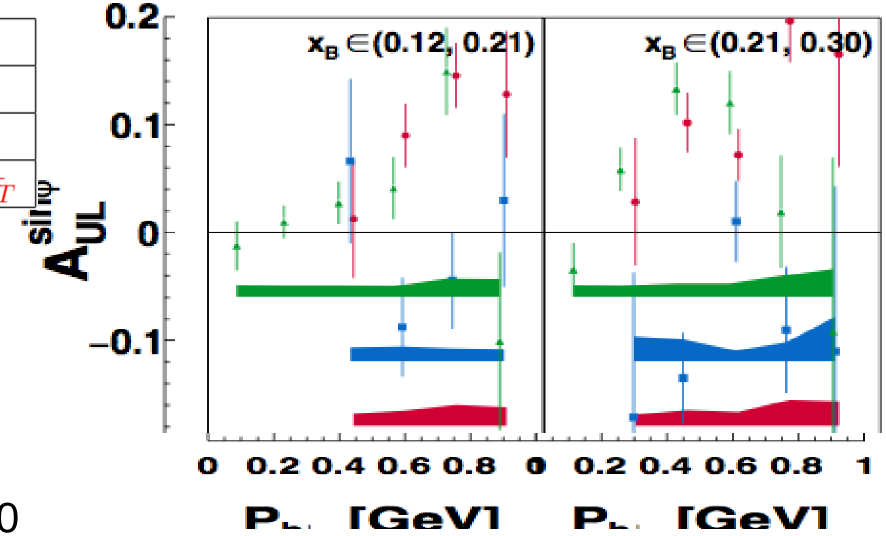

W. Mao & Z.Lu Eur.Phys.J. C73 (2013) 2557

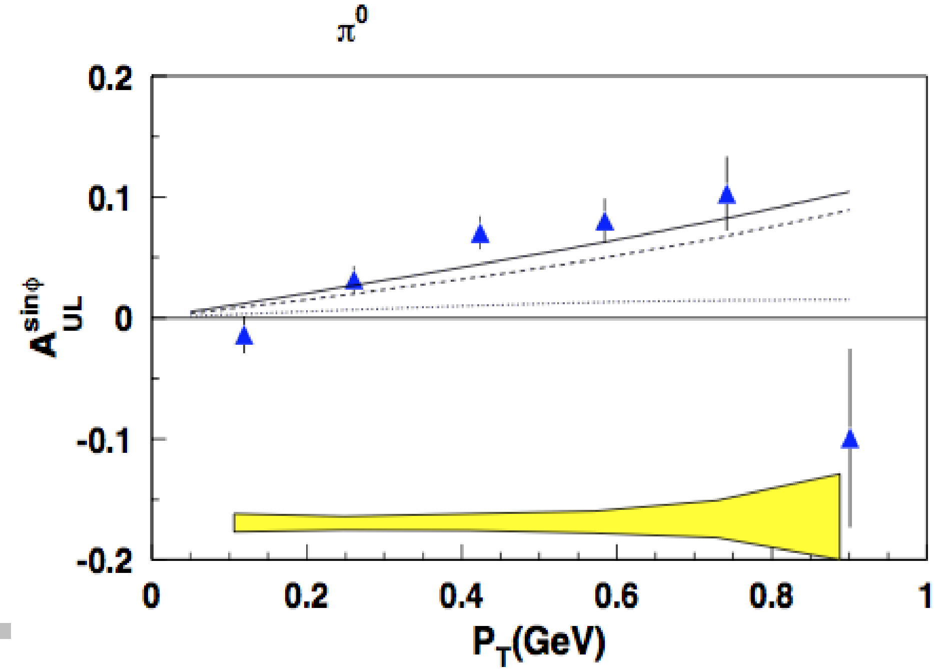

π^0 SSA less sensitive polarized fragmentation effects (Collins function suppressed)

P_T-dependence studies at Hall-C

H. Mkrtchyan(DIS2011)

Experiment E00-108

Beam energy 5.5 GeV

4 cm LH2 and LD2 targets

$$\sigma_d^{\pi^+} \propto (4D^+ + D^-)(u+d)$$

$$\sigma_d^{\pi^-} \propto (4D^- + D^+)(u+d)$$

$$\frac{\sigma_d^{\pi^+}}{\sigma_d^{\pi^-}} = \frac{4D^+ + D^-}{4D^- + D^+}$$

$$D^-/D^+ = (4 - r) / (4r - 1)$$

$$r = \sigma_d(\pi^+)/\sigma_d(\pi^-)$$

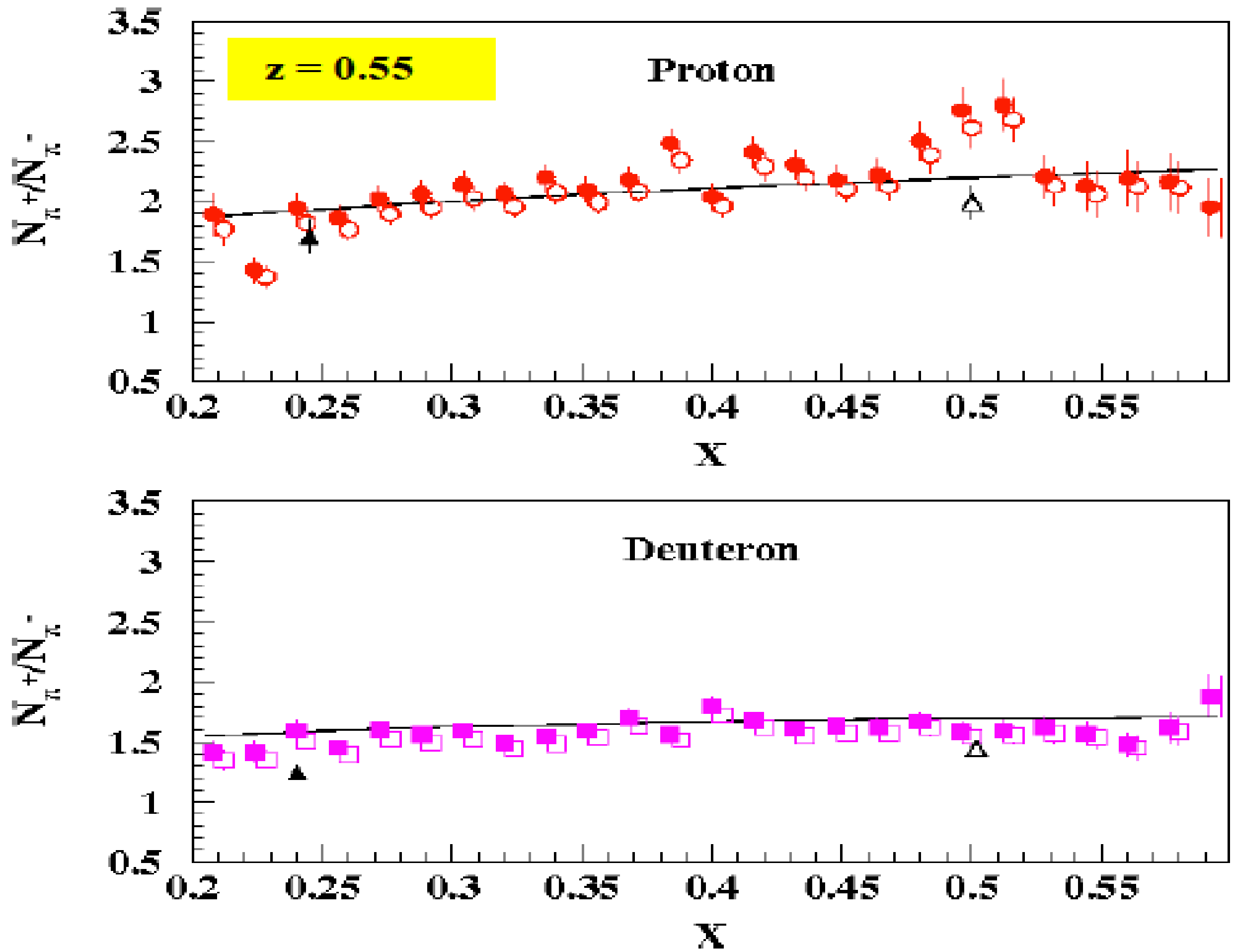

x-dependence of π+/π- ratio is good agreement with the quark parton model predictions (lines CTEQ5M+BKK).

Lattice calculations of HT distributions

N/q	U	L	T
U	$f^{\perp}$	$g^{\perp}$	h ,e
L	$f_L^{\perp}$	$g_L^{\perp}$	h_L ,e_L
T	f_T ,$f_T^{\perp}$	g_T , $g_T^{\perp}$	h_T ,e_T ,$h_T^{\perp}$, $e_T^{\perp}$

(PDFs in terms of Lorenz invariant amplitudes $\tilde{A}_i$
Musch et al, arXiv:1011.1213)

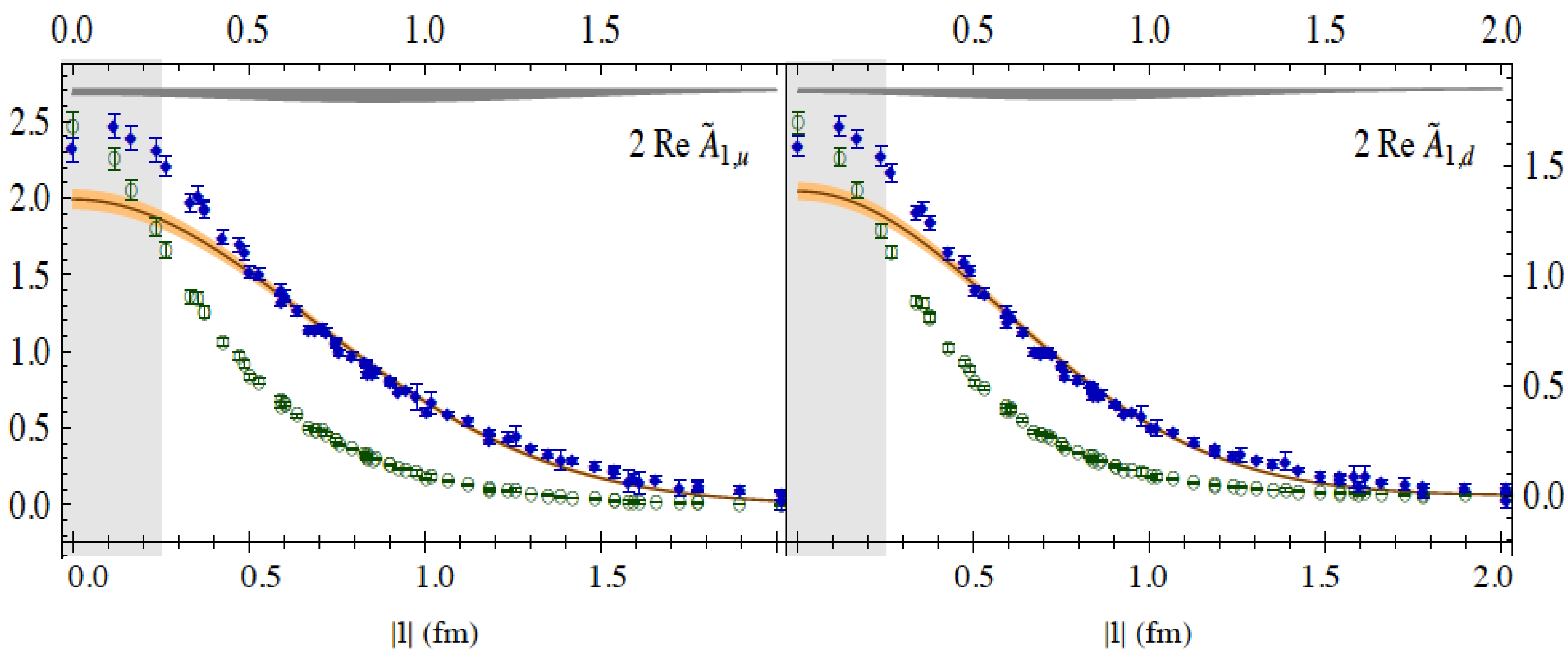

Lattice provides important complementary information on FT for all HT distributions

Azimuthal moments with unpolarized target

quark polarization

N/q	U	L	T
U	$\mathbf{f_1}$		$h_1^{\perp}$
L		$\mathbf{g_1}$	$h_{1L}^{\perp}$
T	$f_{1T}^{\perp}$	g_{1T}	$\mathbf{h_1}$ $h_{1T}^{\perp}$

N/q	U	L	T
U	$f^{\perp}$	$g^{\perp}$	$h, \mathbf{e}$
L	$f_L^{\perp}$	$g_L^{\perp}$	$\mathbf{h_L}, e_L$
T	$f_T, f_T^{\perp}$	$\mathbf{g_T}, g_T^{\perp}$	$h_T, e_T, h_T^{\perp}, e_T^{\perp}$

$$A_{UU}^{\cos\phi} \propto \frac{M_h}{M}\mathbf{f_1}\frac{D^{\perp}}{z} - \frac{M}{M_h} x f^{\perp} D_1$$

q/h	U	L	T
U	$D^{\perp}$	$D_L^{\perp}$	$D_T, D_T^{\perp}$
L	$G^{\perp}$	$\mathbf{G_L^{\perp}}$	$\mathbf{G_T}, G_T^{\perp}$
T	$H, \mathbf{E}$	$\mathbf{H_L}, E_L$	$H_T, E_T, H_T^{\perp}, E_T^{\perp}$

q/h	U	L	T
U	$\mathbf{D_1}$		$D_{1T}^{\perp}$
L		$\mathbf{G_{1L}}$	$G_{1T}^{\perp}$
T	$H_1^{\perp}$	$H_{1L}^{\perp}$	$\mathbf{H_1}$ $H_{1T}^{\perp}$

Azimuthal moments with unpolarized target

quark polarization

N/q	U	L	T
U	$\mathbf{f_1}$		$h_1^\perp$
L		$\mathbf{g_1}$	$h_{1L}^\perp$
T	$f_{1T}^\perp$	g_{1T}	$\mathbf{h_1}$ $h_{1T}^\perp$

N/q	U	L	T
U	$f^\perp$	$g^\perp$	$h, \mathbf{e}$
L	$f_L^\perp$	$g_L^\perp$	$\mathbf{h_L}, e_L$
T	$f_T, f_T^\perp$	$\mathbf{g_T}, g_T^\perp$	$h_T, e_T, h_T^\perp, e_T^\perp$

$$A_{UU}^{\cos\phi} \sim -h_1^\perp \frac{H}{z} + xhH_1^\perp$$

q/h	U	L	T
U	$D^\perp$	$D_L^\perp$	$D_T, D_T^\perp$
L	$G^\perp$	$\mathbf{G_L^\perp}$	$\mathbf{G_T}, G_T^\perp$
T	$H, \mathbf{E}$	$\mathbf{H_L}, E_L$	$H_T, E_T, H_T^\perp, E_T^\perp$

q/h	U	L	T
U	$\mathbf{D_1}$		$D_{1T}^\perp$
L		$\mathbf{G_{1L}}$	$G_{1T}^\perp$
T	$H_1^\perp$	$H_{1L}^\perp$	$\mathbf{H_1}$ $H_{1T}^\perp$

SSA with unpolarized target

quark polarization

N/q	U	L	T
U	$\mathbf{f_1}$		$h_1^\perp$
L		$\mathbf{g_1}$	$h_{1L}^\perp$
T	$f_{1T}^\perp$	g_{1T}	$\mathbf{h_1}$ $h_{1T}^\perp$

N/q	U	L	T
U	$f^\perp$	$g^\perp$	$h, \mathbf{e}$
L	$f_L^\perp$	$g_L^\perp$	$\mathbf{h_L}, e_L$
T	$f_T, f_T^\perp$	$\mathbf{g_T}, g_T^\perp$	$h_T, e_T, h_T^\perp, e_T^\perp$

$$A_{LU}^{\sin\phi} \propto \frac{M_h}{M} \mathbf{f_1} \frac{G^\perp}{z} - \frac{M}{M_h} x g^\perp D_1$$

q/h	U	L	T
U	$D^\perp$	$D_L^\perp$	$D_T, D_T^\perp$
L	$G^\perp$	$\mathbf{G_L^\perp}$	$\mathbf{G_T}, G_T^\perp$
T	$H, \mathbf{E}$	$\mathbf{H_L}, E_L$	$H_T, E_T, H_T^\perp, E_T^\perp$

q/h	U	L	T
U	$\mathbf{D_1}$		$D_{1T}^\perp$
L		$\mathbf{G_{1L}}$	$G_{1T}^\perp$
T	$H_1^\perp$	$H_{1L}^\perp$	$\mathbf{H_1}$ $H_{1T}^\perp$

SSA with unpolarized target

quark polarization

N/q	U	L	T
U	$\mathbf{f_1}$		$h_1^\perp$
L		$\mathbf{g_1}$	$h_{1L}^\perp$
T	$f_{1T}^\perp$	g_{1T}	$\mathbf{h_1}$ $h_{1T}^\perp$

N/q	U	L	T
U	$f^\perp$	$g^\perp$	h, $\mathbf{e}$
L	$f_L^\perp$	$g_L^\perp$	$\mathbf{h_L}, e_L$
T	$f_T, f_T^\perp$	$\mathbf{g_T}, g_T^\perp$	$h_T, e_T, h_T^\perp, e_T^\perp$

$$A_{LU}^{\sin\phi} \sim h_1^\perp \frac{E}{z} + xeH_1^\perp$$

q/h	U	L	T
U	$D^\perp$	$D_L^\perp$	$D_T, D_T^\perp$
L	$G^\perp$	$\mathbf{G_L^\perp}$	$\mathbf{G_T}, G_T^\perp$
T	H, $\mathbf{E}$	$\mathbf{H_L}, E_L$	$H_T, E_T, H_T^\perp, E_T^\perp$

q/h	U	L	T
U	$\mathbf{D_1}$		$D_{1T}^\perp$
L		$\mathbf{G_{1L}}$	$G_{1T}^\perp$
T	$H_1^\perp$	$H_{1L}^\perp$	$\mathbf{H_1}$ $H_{1T}^\perp$

SSA with long. polarized target

quark polarization

N/q	U	L	T
U	$\mathbf{f_1}$		$h_1^\perp$
L		$\mathbf{g_1}$	$h_{1L}^\perp$
T	$f_{1T}^\perp$	g_{1T}	$\mathbf{h_1}$ $h_{1T}^\perp$

N/q	U	L	T
U	$f^\perp$	$g^\perp$	$h, \mathbf{e}$
L	$f_L^\perp$	$g_L^\perp$	$\mathbf{h_L}, e_L$
T	$f_T, f_T^\perp$	$\mathbf{g_T}, g_T^\perp$	$h_T, e_T, h_T^\perp, e_T^\perp$

$$A_{\mathrm{UL}}^{\sin\phi} \propto \frac{M_h}{M}\mathbf{g_1}\frac{G^\perp}{z} + \frac{M}{M_h} x f_L^\perp D_1$$

q/h	U	L	T
U	$D_1^\perp$	$D_L^\perp$	$D_T, D_T^\perp$
L	$G^\perp$	$\mathbf{G_L^\perp}$	$\mathbf{G_T}, G_T^\perp$
T	$H, \mathbf{E}$	$\mathbf{H_L}, E_L$	$H_T, E_T, H_T^\perp, E_T^\perp$

q/h	U	L	T
U	$\mathbf{D_1}$		$D_{1T}^\perp$
L		$\mathbf{G_{1L}}$	$G_{1T}^\perp$
T	$H_1^\perp$	$H_{1L}^\perp$	$\mathbf{H_1}$ $H_{1T}^\perp$

SSA with long. polarized target

quark polarization

N/q	U	L	T
U	$\mathbf{f_1}$		$h_1^\perp$
L		$\mathbf{g_1}$	$h_{1L}^\perp$
T	$f_{1T}^\perp$	g_{1T}	$\mathbf{h_1}$ $h_{1T}^\perp$

N/q	U	L	T
U	$f^\perp$	$g^\perp$	$h, \mathbf{e}$
L	$f_L^\perp$	$g_L^\perp$	$\mathbf{h_L}, e_L$
T	$f_T, f_T^\perp$	$\mathbf{g_T}, g_T^\perp$	$h_T, e_T, h_T^\perp, e_T^\perp$

$$A_{UL}^{\sin\phi} \sim h_{1L}^\perp \frac{H}{z} + x h_L H_1^\perp$$

q/h	U	L	T
U	$D^\perp$	$D_L^\perp$	$D_T, D_T^\perp$
L	$G^\perp$	$\mathbf{G_L^\perp}$	$\mathbf{G_T}, G_T^\perp$
T	$H, \mathbf{E}$	$\mathbf{H_L}, E_L$	$H_T, E_T, H_T^\perp, E_T^\perp$

q/h	U	L	T
U	$\mathbf{D_1}$		$D_{1T}^\perp$
L		$\mathbf{G_{1L}}$	$G_{1T}^\perp$
T	$H_1^\perp$	$H_{1L}^\perp$	$\mathbf{H_1}$ $H_{1T}^\perp$

SSA with unpolarized target

quark polarization

N/q	U	L	T
U	$\mathbf{f_1}$		$h_1^\perp$
L		$\mathbf{g_1}$	$h_{1L}^\perp$
T	$f_{1T}^\perp$	g_{1T}	$\mathbf{h_1}$ $h_{1T}^\perp$

N/q	U	L	T
U	$f^\perp$	$g^\perp$	$h, \mathbf{e}$
L	$f_L^\perp$	$g_L^\perp$	$\mathbf{h_L}, e_L$
T	$f_T, f_T^\perp$	$\mathbf{g_T}, g_T^\perp$	$h_T, e_T, h_T^\perp, e_T^\perp$

$$A_{LL}^{\cos\phi} \sim \frac{M_h}{M} g_{1L} \frac{D^\perp}{z} + x e_L H_1^\perp$$

q/h	U	L	T
U	$D^\perp$	$D_L^\perp$	$D_T, D_T^\perp$
L	$G^\perp$	$\mathbf{G_L^\perp}$	$\mathbf{G_T}, G_T^\perp$
T	$H, \mathbf{E}$	$\mathbf{H_L}, E_L$	$H_T, E_T, H_T^\perp, E_T^\perp$

q/h	U	L	T
U	$\mathbf{D_1}$		$D_{1T}^\perp$
L		$\mathbf{G_{1L}}$	$G_{1T}^\perp$
T	$H_1^\perp$	$H_{1L}^\perp$	$\mathbf{H_1}$ $H_{1T}^\perp$

SSA with unpolarized target

quark polarization

N/q	U	L	T
U	$\mathbf{f_1}$		$h_1^\perp$
L		$\mathbf{g_1}$	$h_{1L}^\perp$
T	$f_{1T}^\perp$	g_{1T}	$\mathbf{h_1}$ $h_{1T}^\perp$

N/q	U	L	T
U	$f^\perp$	$g^\perp$	h, $\mathbf{e}$
L	$f_L^\perp$	$g_L^\perp$	$\mathbf{h_L}$, e_L
T	f_T, $f_T^\perp$	$\mathbf{g_T}$, $g_T^\perp$	h_T, e_T, $h_T^\perp$, $e_T^\perp$

$$A_{LL}^{\cos\phi} \sim \frac{M_h}{M} h_{1L}^\perp \frac{E}{z} + x g_L^\perp D_1$$

q/h	U	L	T
U	$D^\perp$	$D_L^\perp$	D_T, $D_T^\perp$
L	$G^\perp$	$\mathbf{G_L^\perp}$	$\mathbf{G_T}$, $G_T^\perp$
T	H, $\mathbf{E}$	$\mathbf{H_L}$, E_L	H_T, E_T, $H_T^\perp$, $E_T^\perp$

q/h	U	L	T
U	$\mathbf{D_1}$		$D_{1T}^\perp$
L		$\mathbf{G_{1L}}$	$G_{1T}^\perp$
T	$H_1^\perp$	$H_{1L}^\perp$	$\mathbf{H_1}$ $H_{1T}^\perp$

SSA with transversely polarized target

quark polarization

N/q	U	L	T
U	$\mathbf{f_1}$		$h_1^\perp$
L		$\mathbf{g_1}$	$h_{1L}^\perp$
T	$f_{1T}^\perp$	g_{1T}	$\mathbf{h_1}$ $h_{1T}^\perp$

N/q	U	L	T
U	$f^\perp$	$g^\perp$	$h, \mathbf{e}$
L	$f_L^\perp$	$g_L^\perp$	$\mathbf{h_L}, e_L$
T	$f_T, f_T^\perp$	$\mathbf{g_T}, g_T^\perp$	$h_T, e_T, h_T^\perp, e_T^\perp$

$$A_{UT}^{\sin\phi_S} \propto x f_T D_1 - \frac{M_h}{M} x h_T H_1^\perp$$

q/h	U	L	T
U	$D^\perp$	$D_L^\perp$	$D_T, D_T^\perp$
L	$G^\perp$	$\mathbf{G_L^\perp}$	$\mathbf{G_T}, G_T^\perp$
T	$H, \mathbf{E}$	$\mathbf{H_L}, E_L$	$H_T, E_T, H_T^\perp, E_T^\perp$

q/h	U	L	T
U	$\mathbf{D_1}$		$D_{1T}^\perp$
L		$\mathbf{G_{1L}}$	$G_{1T}^\perp$
T	$H_1^\perp$	$H_{1L}^\perp$	$\mathbf{H_1}$ $H_{1T}^\perp$

Twist-3 PDFs : "new testament"

N/q	U	L	T
U	$f^{\perp}$	$g^{\perp}$	h ,e
L	$f_L^{\perp}$	$g_L^{\perp}$	h_L ,e_L
T	f_T , $f_T^{\perp}$	g_T , $g_T^{\perp}$	h_T ,e_T ,$h_T^{\perp}$, $e_T^{\perp}$

$$\frac{1}{2Mx}\,\mathrm{Tr}\left[\tilde{\Phi}_{A\alpha}\,\sigma^{\alpha+}\right] = \tilde{h} + i\,\tilde{e} + \frac{\epsilon_T^{\rho\sigma}\,p_{T\rho}S_{T\sigma}}{M}\left(\tilde{h}_T^{\perp} - i\,\tilde{e}_T^{\perp}\right),$$

$$\frac{1}{2Mx}\,\mathrm{Tr}\left[\tilde{\Phi}_{A\alpha}\,i\sigma^{\alpha+}\gamma_5\right] = S_L\left(\tilde{h}_L + i\,\tilde{e}_L\right) - \frac{p_T\cdot S_T}{M}\left(\tilde{h}_T + i\,\tilde{e}_T\right),$$

$$\frac{1}{2Mx}\,\mathrm{Tr}\left[\tilde{\Phi}_{A\rho}\left(g_T^{\alpha\rho} + i\epsilon_T^{\alpha\rho}\gamma_5\right)\gamma^+\right] = \frac{p_T^{\alpha}}{M}\left(\tilde{f}^{\perp} - i\tilde{g}^{\perp}\right) - \epsilon_T^{\alpha\rho}\,S_{T\rho}\left(\tilde{f}_T + i\tilde{g}_T\right)$$

$$- S_L\,\frac{\epsilon_T^{\alpha\rho}\,p_{T\rho}}{M}\left(\tilde{f}_L^{\perp} + i\,\tilde{g}_L^{\perp}\right) - \frac{p_T^{\alpha}\,p_T^{\rho} - \frac{1}{2}\,p_T^2\,g_T^{\alpha\rho}}{M^2}\,\epsilon_{T\rho\sigma}S_T^{\sigma}\left(\tilde{f}_T^{\perp} + i\tilde{g}_T^{\perp}\right),$$

$$\boxed{\frac{e^{u-d}}{f_1^{u-d}}}$$ a higher twist result from straight links

$\Phi^{[1]} = \frac{m_N}{P^+} e$. (The T-odd term vanishes for straight links)

$\tilde{\Phi}^{[1]} = 2 m_N \tilde{A}_1$

$$\Rightarrow \Phi^{[1]} = \int \frac{d(\ell\cdot P)}{(2\pi)} e^{-ix(\ell\cdot P)} \int \frac{d^2\vec{\ell}_\perp}{(2\pi)^2} e^{i\vec{\ell}_\perp\cdot\vec{k}_\perp} \frac{1}{P^+}\cdot 2 m_N \tilde{A}_1 \Big|_{\ell^+=0}$$

$$= \frac{m_N}{P^+} e$$

$$\Rightarrow e = \int \frac{d(\ell\cdot P)}{2\pi} e^{-ix(\ell\cdot P)} \int \frac{d^2\ell_\perp}{(2\pi)^2} e^{i\vec{\ell}_\perp\cdot\vec{k}_\perp} 2\tilde{A}_1 \Big|_{\ell^+=0}$$

$$\int dx\, e = \int \frac{d^2\ell_\perp}{(2\pi)^2} e^{i\vec{\ell}_\perp\cdot\vec{k}_\perp} 2\tilde{A}_1(\underbrace{\ell^2}_{-\vec{\ell}_\perp^{\,2}}, \underbrace{\ell\cdot P}_{0}) \Big|_{\substack{\ell^+=0\\ \ell\cdot P=0}}$$

$$\int d^2\ell_\perp\, e^{-i\vec{\ell}_\perp\cdot\vec{k}_\perp} e(x,\vec{k}_\perp^{\,2}) = 2\tilde{A}_1(-\vec{\ell}_\perp^{\,2}, 0)$$

use $\ell = -b$

$$\boxed{e^{[1]}(\vec{b}_\perp^{\,2}) = \int_{-1}^{1} dx\, e(x,\vec{b}_\perp^{\,2}) = 2\tilde{A}_1(-\vec{b}_\perp^{\,2}, 0)}$$

so $$\boxed{\frac{e^{[1]}(\vec{b}_\perp^{\,2})}{f_1^{[1]}(\vec{b}_\perp^{\,2})} = \frac{\tilde{A}_1}{\tilde{A}_2}}$$